

# **INVESTIGATION OF ELECTROSTATIC CHARGE IN HOSE LINES**

**INTERIM REPORT  
TFLRF No. 384**

by

**James E. Johnson  
Thomas E. Owen, Ph.D., P.E.  
Scott A. Hutzler**

**U.S. Army TARDEC Fuels and Lubricants Research Facility  
Southwest Research Institute<sup>®</sup> (SwRI<sup>®</sup>)  
San Antonio, TX**

Under Contract to

**U.S. Army TARDEC  
Petroleum and Water Business Area  
Warren, MI**

**Contract No. DAAE-07-99-C-L053 (WD30)**

Approved for public release: distribution unlimited

**October 2006**

### **Disclaimers**

The findings in this report are not to be construed as an official Department of the Army position unless so designated by other authorized documents.

Trade names cited in this report do not constitute an official endorsement or approval of the use of such commercial hardware or software.

### **DTIC Availability Notice**

Qualified requestors may obtain copies of this report from the Defense Technical Information Center, Attn: DTIC-OCC, 8725 John J. Kingman Road, Suite 0944, Fort Belvoir, Virginia 22060-6218.

### **Disposition Instructions**

Destroy this report when no longer needed. Do not return it to the originator.

# INVESTIGATION OF ELECTROSTATIC CHARGE IN HOSE LINES

INTERIM REPORT  
TFLRF No. 384

by  
James E. Johnson  
Thomas E. Owen, Ph.D., P.E.  
Scott A. Hutzler

U.S. Army TARDEC Fuels and Lubricants Research Facility  
Southwest Research Institute® (SwRI®)  
San Antonio, TX

Under Contract to  
U.S. Army TARDEC  
Petroleum and Water Business Area  
Warren, MI

Contract No. DAAE-07-99-C-L053 (WD30)

Approved for public release: distribution unlimited

October 2006

Approved by:



Edwin C. Owens, Director  
U.S. Army TARDEC Fuels and Lubricants  
Research Facility (SwRI)

REPORT DOCUMENTATION PAGE				Form Approved OMB No. 0704-0188	
Public reporting burden for this collection of information is estimated to average 1 hour per response, including the time for reviewing instruction, searching existing data sources, gathering and maintaining the data needed, and completing and reviewing the collection of information. Send comments regarding this burden estimate or any other aspect of this collection of information, including suggestions for reducing this burden, to Washington Headquarters Services, Directorate for Information Operations and Reports, 1215 Jefferson Davis Highway, Suite 1204, Arlington, VA 22202-4302, and to the Office of Management and Budget, Paperwork Reduction Project (0704-0188), Washington, DC 20503.					
1. AGENCY USE ONLY		2. REPORT DATE September 2006		3. REPORT TYPE AND DATES COVERED Final, April 2005 – September 2006	
4. TITLE AND SUBTITLE Investigation of Electrostatic Charge in Hose Lines				5. FUNDING NUMBERS DAAE-07-99-C-L-053 WD 30	
6. AUTHOR(S) Johnson, J.E., Owen, T.E., and Hutzler, S.A.					
7. PERFORMING ORGANIZATION NAME(S) AND ADDRESS(ES) U.S. Army TARDEC Fuels and Lubricants Research Facility (SwRI) Southwest Research Institute P.O. Drawer 28510 San Antonio, Texas 78228-0510				8. PERFORMING ORGANIZATION REPORT NUMBER  TFLRF No. 384	
9. SPONSORING/MONITORING AGENCY NAME(S) AND ADDRESS(ES) U.S. Army TACOM U.S. Army TARDEC Petroleum and Water Business Area Warren, MI 48397-5000				10. SPONSORING/MONITORING AGENCY REPORT NUMBER	
11. SUPPLEMENTARY NOTES					
12a. DISTRIBUTION/AVAILABILITY STATEMENT Approved for public release; distribution unlimited				12b. DISTRIBUTION CODE	
13. ABSTRACT (Maximum 200 words) Current military specifications for collapsible hose used in Army fuel hose line systems, such as the Assault Hose line System (AHS) and the developmental Rapidly Installed Fuel Transfer System (RIFTS) require a means to maintain conductivity/electric bond throughout the length of the hose line. A wire embedded in the hose typically provides this conductive path for static charge to safely dissipate to ground. The need and value for this conductive wire in hose lines have been questioned particularly given the type of fuels used by the military today.  This work provides an engineering assessment, based on experiments and analysis that shows that the RIFTS hose line can be safely operated without a continuous grounding system (bond wire) when operated under conditions for which it was designed. It is also shown that the breakdown potential of the hose is well above voltages generated by the triboelectric effect and thus electrical breakdown is not expected.					
14. SUBJECT TERMS				15. NUMBER OF PAGES	
Electrostatic	Bond	Hose	Jet A1	RIFTS	AHS
Charge	Dissipation	Triboelectric	Testing	Conductivity	Breakdown
				78	
				16. PRICE CODE	
17. SECURITY CLASSIFICATION OF REPORT  Unclassified		18. SECURITY CLASSIFICATION OF THIS PAGE Unclassified		19. SECURITY CLASSIFICATION OF ABSTRACT  Unclassified	
				20. LIMITATION OF ABSTRACT	

## **EXECUTIVE SUMMARY**

The need for a bond system or continuous electrical path attached to collapsible hose used for the transport of fuel as exemplified by the Assault Hose Line System (AHS) and the newly developed Rapidly Installed Fluid Transfer System (RIFTS) has long been questioned. To fully address the perceived need, full-scale experiments based on supporting theoretical arguments have been performed to investigate the electrostatic charging phenomena for collapsible hose and the possibility of exceeding the electrical breakdown potential. Tests were conducted with long hose line segments of the 4-inch diameter AHS hose and the 6-inch diameter RIFTS hose. These tests show that there is little likelihood of exceeding the breakdown voltage of the RIFTS hose when operating at its maximum flow capacity. Furthermore, surface voltages of an unbonded RIFTS hose in contact with the ground will be at the ground potential. It is therefore recommended that no bond wire or continuous electrical path be included on RIFTS hose, which under normal circumstances is in contact with the ground for extended distances.

### **Problem and Objective:**

The implied requirement for a bond system attached to flexible hose lines needs further independent review. The objective of this work is to conduct independent testing and evaluation to assess the potential of a hazardous condition due to electrostatic potential and discharge in military hose lines.

### **Importance of Project:**

Work is considered very important as it addresses Army needs to reduce construction complexities and associated cost of collapsible hose lines while maintaining safety standards.

### **Technical Approach:**

Full-scale experiments were conducted with RIFTS and AHS hoses to characterize electrostatic generation for hose configurations with and without a bond system.

### **Accomplishments:**

Measured surface voltages for the tested hoses were well below the breakdown potential when operated at their maximum flow velocities. A bonding system has no practical use as a means for mitigating electrical breakdown problems. A means for potentially characterizing future hose designs is through its triboelectric charging coefficient.

### **Military Impact:**

The investigation shows that there is no need for a bonding system for RIFTS type of hose and therefore production cost can be reduced for RIFTS and potentially other collapsible hose systems.

## **FOREWORD/ACKNOWLEDGMENTS**

The U.S. Army TARDEC Fuels and Lubricants Research Facility (TFLRF) located at Southwest Research Institute (SwRI), San Antonio, Texas, performed this work during the period May 2005 through September 2006 under Contract No. DAAE-07-99-C-L053. The U.S. Army Tank-Automotive RD&E Center, Petroleum and Water Business Area, Warren, Michigan administered the project. Mr. Luis Villahermosa (AMSTA-RBFF) served as the TARDEC contracting officer's technical representative. Mr. Anthony Mercieca and Mr. Steve Moyer, U.S. Army RDECOM, provided technical advise and program direction. The Petroleum and Water Department, U.S. Army Quartermaster Center and School, Fort Lee, Virginia provided a test site and support during the test of hose lines.

Special acknowledgement is given to the entire staff of U.S. Army Fuels and Lubricants Facility (SwRI) for dedication and support in conducting this extensive program. Special thanks for their technical support and dedication goes to Dr. Tom Owen (Consultant, Owen Engineering Services), James R. Johnson, Jr., Daniel Anctil, and Dolores Hobart.

# TABLE OF CONTENTS

Section	Page
<b>1.0 OBJECTIVE</b> .....	<b>1</b>
<b>2.0 OVERVIEW OF RESEARCH PROGRAM</b> .....	<b>1</b>
<b>3.0 Set Up of Field Test Site</b> .....	<b>2</b>
3.1 Test Site and Test Hoses.....	2
3.1.1 Location.....	2
3.1.2 Test Hose.....	3
3.2 Configurations and Instrumentation of Flow Loops.....	3
3.2.1 General Experiment Considerations.....	4
3.2.2 Loop Configuration for December 2005 Tests.....	7
3.2.2.1 Loop Components.....	7
3.2.2.2 Loop Layout.....	7
3.2.2.3 Fabricated Components.....	12
3.2.2.4 Instrumentation and Data Acquisition.....	13
3.2.2.4.1 Streaming Current Measurement.....	15
3.2.2.4.2 Electrostatic Field Strength Measurement.....	16
3.2.2.4.3 Measurement of Flow, Fuel Temperature, and Pressure.....	17
3.2.2.4.4 Listing of Instruments.....	18
3.2.2.4.5 Installation of Test Loop at Fort Lee (December Tests).....	19
3.2.3 Loop Configuration for August 2006 Tests.....	20
3.2.3.1 Pump Station Change.....	21
3.2.3.2 Additional Streaming Current Section.....	21
3.2.3.3 RIFTS Hose – 500 Feet.....	23
<b>4.0 Hose Configurations and Flow Conditions</b> .....	<b>24</b>
<b>5.0 Electrostatics For Flexible Conduit</b> .....	<b>25</b>
5.1 Flexible Fuel Hose Electrostatics Problem.....	25
5.2 Triboelectric Charging and Discharge of Dielectric Liquids in Pipe Flow.....	26
5.2.1 Electrostatic Charging Phenomena.....	26
5.2.2 Charge Dissipation Phenomena.....	28
5.2.3 Electrostatic Hazards Related to Collapsible Fuel Hoses.....	30
5.2.3.1 Charge Delivery.....	30
5.2.3.2 Electrostatic Potential.....	30
<b>6.0 Measurement of Electrostatic Parameters</b> .....	<b>32</b>
6.1 Measurement of Streaming Current in Flexible Fuel Hoses.....	32
6.1.1 Theoretical Considerations.....	32
6.1.2 Flow Loop Checkout and Calibration.....	34
6.1.3 Measurement and Analysis of Streaming Current.....	36
6.2 Measurement of Electrostatic Potential on Flexible Fuel Hoses.....	38
6.3 Fuel Hose Dielectric Breakdown.....	41
<b>7.0 Fort Lee Field Tests</b> .....	<b>43</b>
7.1 Experimental Field Test Data and Analysis.....	43
7.1.1 December 2005 Field Tests.....	44
7.1.1.1 Streaming Current Measurements in the RIFTS Fuel Hose.....	44
7.1.1.2 Streaming Current Measurements in the AHS Fuel Hose.....	48
7.1.2 August 2006 Field Tests.....	51
7.1.2.1 Streaming Current Measurements in the RIFTS Fuel Hose.....	51
7.1.2.2 Fuel Flow Loop Checkout Test.....	56
7.1.2.3 Electrostatic Potential Measurements on the RIFTS Fuel Hose.....	57
7.1.2.4 Laboratory Tests of Fuel Hose Dielectric Strength and Breakdown Voltage.....	60
7.2 Discussion of Field Test Results.....	61

7.2.1	Streaming Current Tests .....	61
7.2.2	Electrostatic Hose Potential Tests.....	63
<b>8.0</b>	<b>CONCLUSIONS AND RECOMMENDATIONS .....</b>	<b>64</b>
8.1	Summary .....	64
8.2	Conclusions .....	65
8.3	Recommendations for Future Work .....	66
<b>9.0</b>	<b>REFERENCES .....</b>	<b>67</b>
9.1	SUPPLEMENTAL REFERENCES.....	67

## LIST OF TABLES

<b>Table</b>	<b>Page</b>
Table 1. Test Variable and Quantification Method .....	18
Table 2. Hose Configurations and Flow Conditions for August Tests .....	25
Table 3. Fuel Hose Dielectric Strength and Breakdown Voltage.....	60

## LIST OF FIGURES

<b>Figure</b>	<b>Page</b>
Figure 1. Loop Layout and Itemized List Of Components .....	8
Figure 2. Layout of Flow Loop Components in Tank 2.....	11
Figure 3. Charge Bleed-Off Tank, Valve, Measurement Section, and Isolators .....	12
Figure 4. Photo of Butterfly Valve Connected to Isolator Section and Single Groove Transition. ....	13
Figure 5. Photo of Instrumentation Cart .....	13
Figure 6. Diagram of Instrumentation and Data Acquisition System .....	14
Figure 7. Streaming Current Measurement Section .....	15
Figure 8. Diagram of Electrostatic Field Sensor and Photographs of Shield System for 6-Inch Hose.....	16
Figure 9. Calibration Fixture - Field Sensor is Mounted in the Center.....	17
Figure 10. Fuel Flow, Temperature, and Pressure Measurement Section .....	18
Figure 11. Photos of the Installation as Assembled for the December 2005 Tests .....	20
Figure 12. Installation of Tandem Streaming Current Sections .....	21
Figure 13. Loop Layout for August 2006 Tests .....	22
Figure 14. Field Setup for August Tests Showing Bridge Between Tanks, Pump And Bladder Arrangement, and Views Of 6" RIFTS Hose On Electrical Isolators.....	23
Figure 15. Relative Charge Decay Versus Time for Hydrocarbon Fuels .....	29
Figure 16. Flow-Line Charge Measuring Section Geometry and Electrical Connections .....	32
Figure 17. Flow-Line Measuring Setup for Testing Fuel Hoses.....	37
Figure 18. Coaxial Fuel Hose and Surrounding Grounded Metallic Cylinder .....	39
Figure 19. Net Relaxation Current in RIFTS Hose – Test Run 1 (Dec. 2005).....	45
Figure 20. Net Relaxation Current in RIFTS Hose – Test Run 2 (Dec. 2005).....	45
Figure 21. Reynolds Number – RIFTS Hose, Jet A1 Fuel – (Dec. 2005).....	46
Figure 22. Streaming Current in RIFTS Fuel Hose – Test Run 1 (Dec. 2005).....	46
Figure 23. Streaming Current in RIFTS Fuel Hose – Test Run 2 (Dec. 2005).....	47
Figure 24. Triboelectric Charging Coefficient – RIFTS Fuel Hose (Dec. 2005).....	47
Figure 25. Net Relaxation Current in AHS Hose – Test Run 1 (Dec. 2005).....	49
Figure 26. Net Relaxation Current in AHS Hose – Test Run 2 (Dec. 2005).....	49
Figure 27. Reynolds Number – AHS Hose, Jet A1 Fuel – (Dec. 2005).....	49
Figure 28. Streaming Current in AHS Fuel Hose – Test Run 1 (Dec. 2005).....	50
Figure 29. Streaming Current in AHS Fuel Hose – Test Run 2 (Dec. 2005).....	50
Figure 30. Triboelectric Charging Coefficient – AHS Fuel Hose (Dec. 2005).....	51
Figure 31. Net Relaxation Current in RIFTS Hose – Test Run 1 (Aug. 2006).....	52
Figure 32. Net Relaxation Current in RIFTS Hose – Test Run 2 (Aug. 2006).....	52
Figure 33. Net Relaxation Current in RIFTS Hose – Test Run 3 (Aug. 2006).....	53
Figure 34. Net Relaxation Current in RIFTS Hose – Test Run 4 (Aug. 2006).....	53

Figure 35. Reynolds Number – RIFTS Hose, Jet A1 Fuel – (Aug. 2006).....	53
Figure 36. Streaming Current in RIFTS Fuel Hose – Test Run 1 (Aug. 2006) .....	54
Figure 37. Streaming Current in RIFTS Fuel Hose – Test Run 2 (Aug. 2006) .....	54
Figure 38. Streaming Current in RIFTS Fuel Hose – Test Run 3 (Aug. 2006) .....	55
Figure 39. Streaming Current in RIFTS Fuel Hose – Test Run 4 (Aug. 2006) .....	55
Figure 40. Triboelectric Charging Coefficient – RIFTS Fuel Hose (Aug. 2006).....	56
Figure 41. Residual Charge Density Entering the Hose Test Section .....	57
Figure 42. Field Meter Calibration Curve for Potential Measurements on the RIFTS Fuel Hose .....	58
Figure 43. Electrostatic Potential at Four Test Positions on the RIFTS Flexible Fuel Hose .....	59
Figure 44. Electrostatic Potential along the RIFTS Hose for Four Fuel Flow Velocity Test Conditions .....	60
Figure 45. Comparison of Streaming Currents Generated in the RIFTS and AHS Flexible Fuel Hoses (Dec. 2005 Tests).....	61
Figure 46. Comparison of Streaming Currents in the RIFTS Hose Tests Conducted in December 2005 and in August 2006.....	62
Figure 47. Measured and Predicted Streaming Current in the RIFTS Hose for the Change in Fuel Conductivity.....	63

## **SYMBOLS AND ABBREVIATIONS**

AHS	Assault Hose Line System
IPDS	Inland Petroleum Distribution System
RIFTS	Rapidly Installed Fluid Transfer System
SwRI	Southwest Research Institute
TARDEC	U.S. Army Tank-automotive RD & E Center
TFLRF	U.S. Army TARDEC Fuels and Lubricants Research Facility

**BLANK PAGE**

## **1.0 OBJECTIVE**

Current military specifications for collapsible hose used for Army fuel hose line systems, such as the Assault Hose line System (AHS) and the developmental Rapidly Installed Fluid Transfer System (RIFTS) require continuous electrical connectivity throughout the length of the hose line. A conductive material such as a copper wire embedded or physically attached to the surface of the hose, known as an electrical bond, provides a path for the static charge to dissipate to ground. The need and value of this conductive material in hose lines have been questioned given the types of fuels used by the military and because these hoses generally are in contact with the ground for exceptionally long distances and have sufficient time to dissipate charge.

The objective of this work is to conduct independent testing and evaluation to assess the potential of a hazardous condition due to electrostatic potential and discharge in military hose lines. An objective source of data and information will provide a basis for sound engineering recommendations for safe design and operations of bulk fuel distribution systems.

## **2.0 OVERVIEW OF RESEARCH PROGRAM**

Electrostatic charging of hydrocarbon fuels is a naturally occurring phenomenon associated with the transport of fuel in a conduit. This charge can accumulate in storage tanks and similar vessels where an electrostatic discharge could, if strong enough, ignite fuel vapors. The charging process also gives rise to high voltages that are impressed across the carcass of the hose, and if these voltages exceed the electrical breakdown voltage of the hose, then intense discharging can occur resulting in the formation of pinholes in the hose wall.

While the basic principles of charge generation are fairly well established, the prediction of voltages and charge magnitude prove to be rather imprecise due primarily to the lack of detailed knowledge of the interaction of numerous variables. Full scale testing of conduits with representative fluids is generally required to precisely characterize charging phenomena. To investigate electrostatic charging of collapsible hose lines, tests were conducted on two separate occasions at Fort Lee. The test hoses included the 6.2-inch inside diameter RIFTS hose and the 4-inch diameter AHS hose. Hose lengths ranged from 500 to 1000 feet.

The tests were designed specifically to generate maximum voltages resulting from the charging process. This is accomplished by electrically isolating the entire length of test hose, flowing fuel at velocities much higher than intended for the hose, and by using a hydrocarbon fuel of the lowest possible electrical conductivity. The test fluid for these tests was Jet A1 with no additives. Test results shows that both RIFTS and AHS hose generate voltages across the hose carcasses that are well below the breakdown values. This proved to be true for worn RIFTS hose also.

One of the main assumptions regarding charge bleed off is that when bondless RIFTS and AHS hoses rest on the ground they will have sufficient contact area and length of time to dissipate charge and thus the hose wall will be a ground potential. This assumption proved to be correct

and is the main basis for recommending that bond systems can be omitted from production hoses that are used for long distance fluid transfer. It is important to recognize that an impressed voltage across the carcass will be generated whether or not a bond is installed, or whether or not the hose is in contact with the ground.

Section 3 of this report provides complete details of how the tests were setup and how the data were acquired, and Section 4 describes hose configurations and flow conditions. Section 5 provides theoretical background for electrostatics related to hoses and Section 6 develops the basis for properly reducing the test data into meaningful engineering results. Section 7 presents the analysis of the field data. Sections 5 and 6 need not be studied in great detail as a prerequisite for understanding Section 7. Conclusions and Recommendations are presented in Section 8.

This research was accomplished over the period of April 2005 through October 30, 2006.

### **3.0 Set Up of Field Test Site**

Full scale testing is required to acquire reliable and relevant information needed for characterizing electrostatic generation and dissipation phenomena associated with collapsible hoses. These full-scale tests also need to be conducted with a kerosene-based fuel so that proper boundary layer activity at the hose wall is fully captured in the test results. There are relatively few installations setup for safely accommodating an experimental set up of the type required for these experiments. One appropriate site is Fort Lee, VA where field training for the transportation and storage of fuel is conducted. This section describes the experimental setup and Section 4.0 describes the test conditions. Section 5.0 highlights the electrostatic theory used to guide the experiments and Section 6.0 discusses the measurement of electrostatic parameters. The results of the testing are discussed in Section 7.0 followed by conclusions and recommendations in Section 8.0.

#### **3.1 Test Site and Test Hoses**

##### **3.1.1 Location**

Fort Lee VA was chosen as the test site and in particular, the Petroleum Training Facility provided the necessary features for testing, which primarily includes equipment needed for fuel handling and spill containment. Concrete revetments that normally provide spill containment for a large 42-foot diameter storage vessel and an adjacent general-purpose revetment were utilized to likewise provide spill containment for the flow loops.

To accommodate the long length of test hose in a safe manner, it is placed in a concrete revetment, also know as a tank. The particular tank utilized is know as “Tank 2” (132 feet by 132 feet) identified on a drawing titled “Pump Station and Secondary Containment Grading and Drainage Plan,” Petroleum Training Facility Fort Lee, Virginia, Project No.225070, Sheet C-9.

The adjacent tank known as “Tank 1” (88 feet by 88) was used for placement of a 600 GPM pump (Model US690ACD-1), 20K gallon collapsible bag, and interconnecting hose. A distance of approximately 40 feet separates these tanks and therefore the flow loop must bridge across the gap between tanks.

Fort Lee also provided field equipment needed for installation of the test loop, which included cranes and operators, and manpower to place equipment and hoses.

### **3.1.2 Test Hose**

The RIFTS hose and AHS hose are representative hose lines that are considered truly flexible and collapsible. These hoses are non-metallic and therefore exhibit a propensity for collecting charge. Both hose systems represent current or developmental technologies used by the Army.

The RIFTS conduit is fabricated based on conventional woven hose technology and it is made of several reinforcement layers known as jackets, and thus the RIFTS hose is considered a “jacketed hose.” The innermost layer of the conduit is the inner bladder, which must resist the effects of the various fuels. This layer is a polyester fiber reinforced bladder consisting of a circular woven, all polyester jacket through which a thermoplastic polyurethane (TPU) has been extruded. This forms a composite bladder in which the TPU completely encases the polyester reinforcement and eliminates any chance of delamination of the inner bladder. The second and third layers of the hose act as the structural members of the hose and are constructed of Aramid yarns and are not coated. Aramid is used in both structural members of the hose; warp and weft. The fourth, or outer, jacket is polyester with a urethane emulsion coating, is intended to protect the Aramid jackets, and is not a structural member. The application of a urethane emulsion topcoat is used to effectively seal the fabric from the ingress of foreign materials as well as reducing the amount of water or fuel that may be absorbed into the hose conduit. When the hose is pressurized, its nominal inside diameter is 6.2 inches and the hose wall consisting of the four jackets is approximately 0.35 inches thick. The RIFTS hose is considered to be a high-pressure hose with a rated pressure exceeding 600 psi. The RIFTS hose is a product of Niedner, Coaticook, QC, Canada.

The AHS hose is considered a “through the weave” extruded hose. Its construction technique is similar to the RIFTS inner bladder. However, the AHS hose is more monolithic in the sense that the extruded plastic material is continuous through the entire thickness of the hose wall. The nominal inside diameter is 4.0 inches with a wall thickness of approximately 0.3 inches. The working pressure of the AHS hose is 150 psi. The AHS hose is a product of LaBarge Products Inc., St. Louis, MO, USA.

## **3.2 Configurations and Instrumentation of Flow Loops**

The initial plan was to conduct the entire test program in one outing over a two-week time span in late November and early December 2005. Due to inclement weather conditions, pumping difficulties, and less than desirable performance of an electrostatic field instrument, a second

expedition was planned and carried out in August 2006. However, valuable test data was obtained during the December tests, which was further supplemented by accurate electrostatic field measurements obtained during the August tests. This report provides comprehensive data and analysis from both test events.

General features required for the flow loop (December and August configurations) are highlighted below.

- Ability to pump Jet A1 safely,
- Maximum operating pressure of 150 psi,
- Installation of 500 to 1000 feet of 4" dia. AHS test hose,
- Installation of 500 to 1000 feet of 6" dia. RIFTS test hose,
- Flow velocity up to or exceeding 10 ft/sec in all test hoses,
- Ability to electrically isolate the test hose from other parts of the loop,
- Ability to electrically isolate the test hose from ground (floor of revetment),
- Real time data acquisition for recording of:
  - Fuel flow rate
  - Fuel temperature
  - Streaming current (upstream and down stream of the test hose)
  - Electrostatic fields (numerous locations along the test hose),
- Specialized charge dissipation vessels for controlling charge buildup
- Inclusion of 'measurement sections' for measuring streaming current,
- Inclusion of an electrostatic field sensor, and
- Off line measuring instruments for humidity, electrical isolation, fuel electrical conductivity, and fuel pressure.

The major differences between the configurations of December and August are:

- Two pumps used in August configuration compared to one in December,
- Only test hose for August tests was 500 feet of RIFTS hose,
- Improved field instrumentation for August tests, and
- Improved streaming current calibration setup for the August configuration.

### **3.2.1 General Experiment Considerations**

The general requirements for a practical experimental setup for testing electrostatic charging in flexible fuel hoses that were incorporated into the Fort Lee tests are:

#### **(1) *Relaxation Current Measurements***

Fuel parcel transit time through the measuring sections must be sufficiently long to allow useful levels of relaxation current to be measured at the highest flow rates of interest. This condition is achieved by making the internal volume of the measuring section large enough that the residence time of a

fuel parcel is comparable with the relaxation time constant of the fuel being tested. Otherwise, the measured relaxation current must be compensated for the finite residence time of the charged fuel.

**(2) *Minimum Measuring Section Triboelectric Charging***

Triboelectric charging in the measuring sections at the maximum fuel flow rates of interest must be small compared with the true relaxation current to be measured in the hose test loop. This requirement is achieved by reducing the boundary layer fuel velocity by suitable design of the measuring section.

**(3) *Matched Fuel Flow Patterns in Measuring Sections***

Theoretical considerations for accurate data analysis indicate that the two measuring sections should be as identical as possible in their response to fuel relaxation current measurements. In addition to identical internal volumes, this requirement also pertains to the internal fuel flow patterns within the measuring sections with and without the test specimen installed. In practice, this requirement can be achieved by making the inlet and outlet apertures of the upstream and downstream measuring section insulators the same diameter as that of the flow line to be tested. When the internal fuel circulation flow patterns in the two measuring sections are well balanced and the throughput transit time is comparable with the fuel relaxation time constant, the measurement system calibration will be essentially independent of the fuel volume flow rate.

**(4) *Buffer Storage Tanks***

The use of buffer storage tanks can eliminate the effects of extraneous charging effects in the pumps, filters, and other parts of the flow loop test setup. These tanks are relatively small in size, typically 150 gal capacity, and must be designed to withstand the flow line pressures used in the tests. When the fuel residence time is long, typically characterized by a fuel parcel transit time greater than about four times the relaxation time constant of the fuel, and the tank is grounded, the electrostatic charge exiting the tank will be a negligibly small fraction of the charge generated in the test hose flow loop. Therefore, measurements of streaming currents downstream of the test hose can be attributed to the hose only.

**(5) *Hose Electrostatic Field and Potential Measurements***

The electric field surrounding the hose must be measured with the entire length of the hose test section insulated above ground. This can be accomplished by inserting short lengths of clean 4-in. diameter PVC pipe under the hose at approximately 5-ft. intervals. At this support interval, the stiffness of the hose will be sufficient to prevent excessive sagging when the hose is filled with fuel and operated at the intended flow rates and pressures. For an average insulator spacing of five feet, the number of supports is  $L_{\text{hose}}(\text{ft})/5(\text{ft})$ , corresponding to 100 supports per 500-ft length of hose. The quality of the supporting insulators must be exceptionally high (surfaces free of contaminating dirt and moisture films) to minimize shunt leakage resistance distributed along the test hose. The external surface of the hose will be somewhat conductive because of dust and moisture embedded in the polymer fabric outer jacket. Touching the operating hose in this insulated condition will impart a mild electrical shock and, if the hose is touched while measuring the electric field, such inadvertent discharges will tend to drain the surface image charge normally equilibrated on the outside surface of the hose, reducing the observed field reading at any position along the hose. When the static equilibrium of the charged hose is disturbed, a certain time interval will be required before equilibrium is re-established. The time constant required for restoring equilibrium is governed by the total leakage resistance of the supporting insulators and the capacitance of the isolated hose test section relative to ground, with some additional influence related to the humidity of the air surrounding the hose.

**(6) *Electrostatic Instrumentation***

Two DC ammeters having sufficient sensitivity to allow accurate measurements of currents in the picoampere range are required for measurements of the expected measuring section relaxation currents. For measurements of the expected electrostatic potential on the test hose, a non-contact electric field meter capable of measuring fields up to about 10 or 20 kV/cm is required. This measurement range is dependent on the annulus spacing between the hose and the grounded metallic shell in which the sensor probe is mounted.

**(7) *Fuel***

Jet A1 diesel fuel is recommended for use in the planned flow-loop flexible hose electrostatic tests. Jet A1 fuel is free of any static dissipator dopant and, therefore, has the lowest electrical

conductivity of all diesel fuels (typically as low as 1-2 pS/m). By using this fuel, the electrostatic streaming currents and hose potentials can be expected to be to reach their worst-case conditions and thereby exaggerate the observed electrostatic phenomena that might occur when using other fuels having higher electrical conductivity.

### **3.2.2 Loop Configuration for December 2005 Tests**

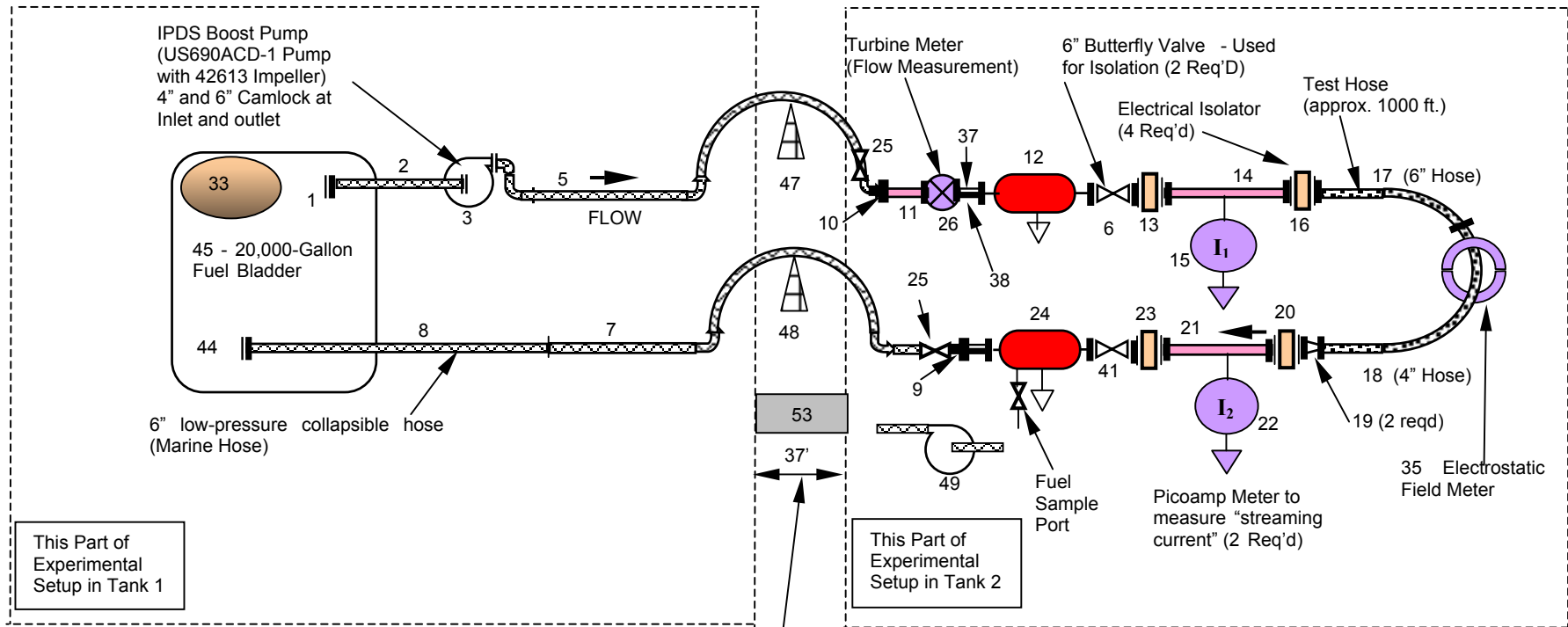
#### **3.2.2.1 Loop Components**

Components for the loop consisted of a combination of government furnished items (GFE) and components designed and fabricated specifically for the flow loop. GFE items included the loop 600 GPM pumps, 20,000 gallon collapsible fuel bladder, approximately 7,500 gallons of Jet A1 fuel (without additives), interconnecting 6" marine hose with appropriate camlock fittings, a bridge between Tanks 1 and 2, small fuel transfer pump, three six foot sections of IPDS aluminum pipe, and numerous interconnecting fittings (Victaulic). SwRI designed and fabricated two charge bleed off tanks (135 gallon capacity each), assembled the instrumentation equipment, provided above ground isolation supports for the hose, and fabricated electrical isolators that were installed at various locations along the loop. The RIFTS test hose was made available from the RIFTS program and LaBarge Products, Inc shipped in the AHS hose with fittings.

#### **3.2.2.2 Loop Layout**

The arrangement of components used in the flow loop is shown in Figure 1 and the arrangement of 1000 feet of test hose within the large revetment (Tank 2) is shown in Figure 2.

As shown, the loop is a closed loop where fuel is pumped from a reservoir (collapsible bladder) through the test hose and then returned to the reservoir. Also, while only one path for the 1000 feet of hose is shown in Figure 2, both the 4" AHS hose and 6" RIFTS hose were laid side by side (but not touching) along this path. Sufficient cooling of the loop is provided by the 7,500 gallons of fuel within the bladder, although the fuel does heat up when the loop is in operation. The heat up is monitored during testing and the fuel was not allowed to exceed approximately 110°F.



█ = 6" Victaulic Coupling with seal, IPDS style, 16 required, item 46

**Standby Equipment**

Item	Description
4	4" IPDS ell (2)
36	IPDS vent (2)

**Figure 1. Loop Layout and Itemized List Of Components**

Listing of Components Corresponding to Figure 1 – (November 23, 2005)

Item	Description	No. Reqd	Source	Comments
1	4" cam-lock 90° elbow	1	Govt.	Use existing 4" suction line at Ft. Lee
2	"6 suction hose, Camlock end fittings, low pressure, 10'+ length	1	Govt.	Links tank to boost pump inlet hose
3	IPDS Boost Pump (US690ACD-1)	1	Govt.	
4	IPDS 6"-90° ell, single grooved (rated for 720 psi)	2	Govt.	Have on hand in case needed
5	Marine Hose – 6" Diameter with Camlock fittings, 50+ <del>feet</del>	1	Govt.	Length to reach between pump and 6 (~50')
6	6" Butterfly valve, wafer type	1	SwRI	Used to isolate hose
7	Marine Hose – 6" Diameter with Camlock fittings, 30+ <del>feet</del>	1	Govt.	Connects Marine hose to item 25
8	Marine Hose – 6" Diameter with Camlock fittings, 30+ <del>feet</del>	1	Govt.	Connects Marine hose to item 44 and 25
9	6" IPDS single groove to 6" Camlock (male)	1	SwRI	
10	6" IPDS single groove to 6" Camlock (female)	1	SwRI	
11	6' section of IPDS Al pipe, grooved ends, rated 720 psi.	1	Govt.	
12	135 Gallon Tank (6" SG one end, 6"-150# flg one end, sample port and drain)	1	SwRI	Fabricated by SwRI
13	Electrical Isolator (includes 6"-150# flg to single groove adapter)	1	SwRI	Fabricated by SwRI
14	6' section of IPDS Al pipe, grooved ends, rated 720 psi.	1	Govt.	
15	Picoamp meter	1	SwRI	Used to measure streaming current
16	Electrical Isolator (includes 2 – 6"-150# flg to single groove adapters)	1	SwRI	Fabricated by SwRI
17	6" RIFTS Hose, single groove fittings, Niedner [This is the Test Article]	1000'	SwRI	To borrow from RIFTS inventory
18	4" AHS, special fittings, LaBarge [This is the Test Article]	1000'	Govt.	Supplied by LaBarge
19	Adapter, 6"-150# flg to 4" AHS fitting (used when 4" hose installed)	2	SwRI	Designed and fabricated by SwRI
20	Electrical Isolator (includes 2 – 6"-150# flg to single groove adapters)	1	SwRI	Fabricated by SwRI
21	6' section of IPDS Al pipe, grooved ends, rated 720 psi.	1	Govt.	
22	Picoamp meter	1	SwRI	Used to measure streaming current
23	Electrical Isolator (includes 6"-150# flg to single groove adapter)	1	TBD	Supplied by SwRI
24	135 Gallon Tank (6" SG one end, 6"-150# flg one end, sample port and drain)	1	SwRI	Fabricated by SwRI
25	6" Gate valve with Camlock fittings	2	Govt.	Used for backpressure and isolation
26	6" Turbine meter with 6" IPDS Single groove ends	1	SwRI	Purchased by SwRI for Govt
27				
28				
29				
30				
31				
32				
33	Jet Al – approx 7500 gallons in a 20K bladder	Lot	Govt.	



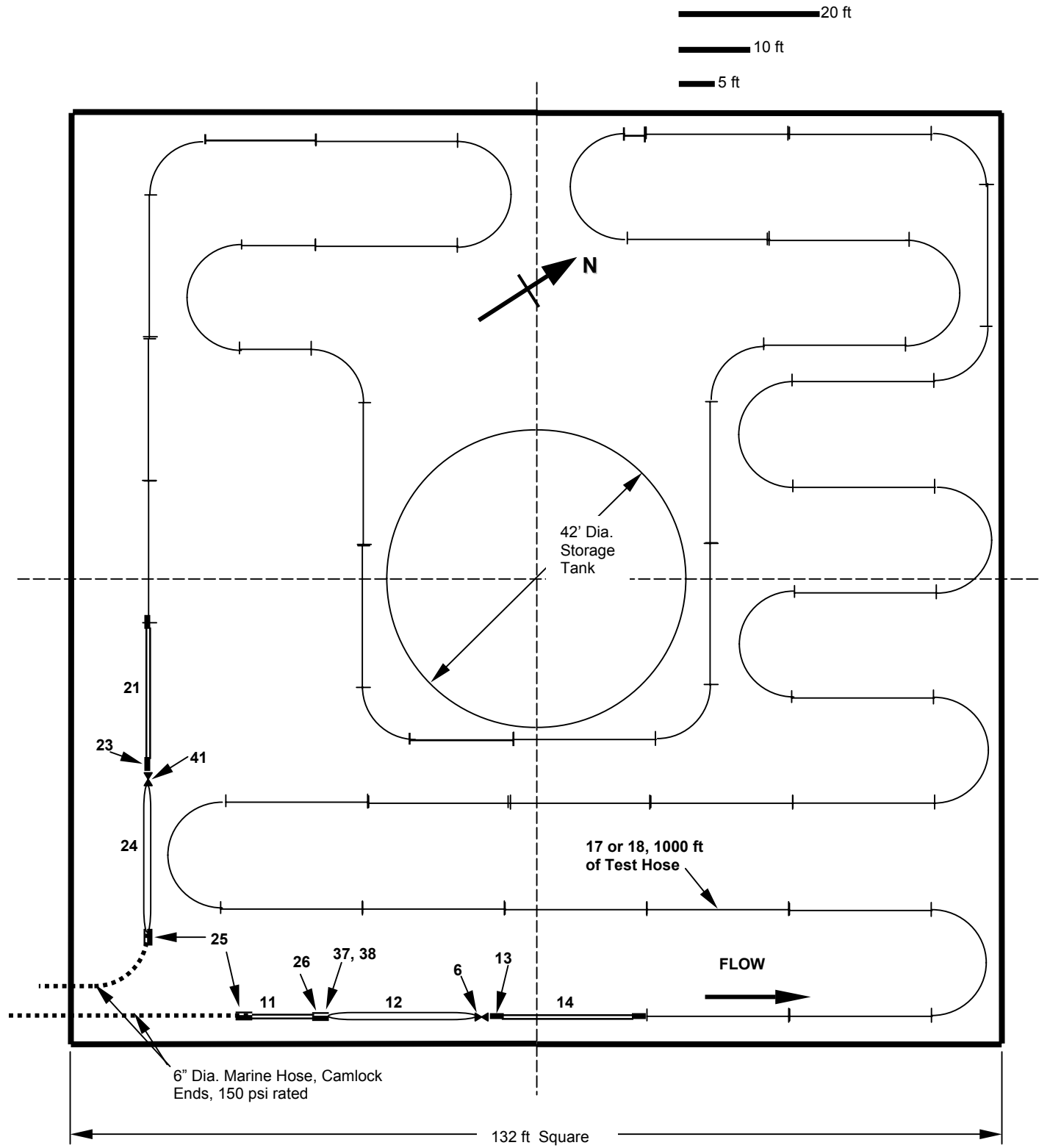


**Figure 2. Layout of Flow Loop Components in Tank 2**

### 3.2.2.3 Fabricated Components

Figure 3 shows the physical layout of a charge bleed off tank and streaming current measurement section. The item numbers refer to those used in Figure 1. This unit is required at the upstream end of the test hose and a matching unit is required at the downstream end of the hose. The bleed off tank is used to clear charge from the fuel prior to entry into the hose and likewise a bleed off tank is required to clear charge generated in the test hose so that charge free fuel is returned to the pump and reservoir.

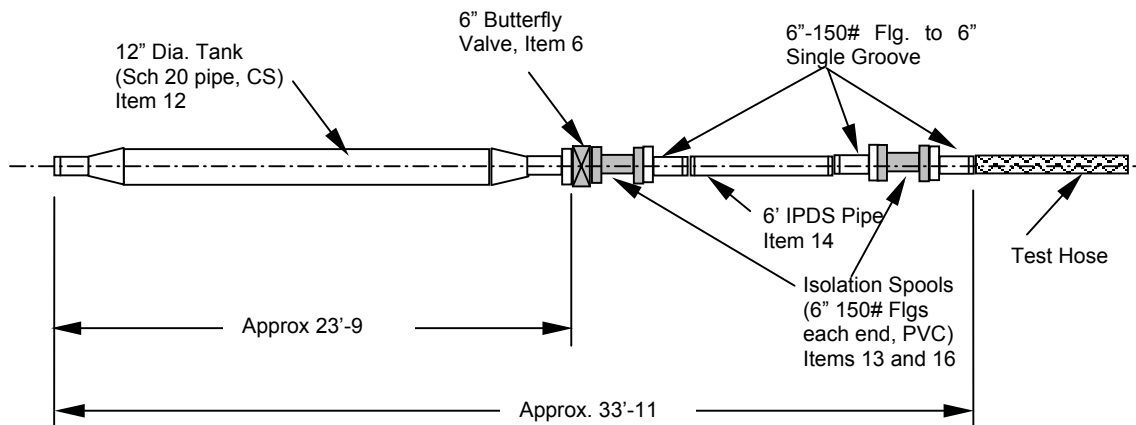


**Figure 3. Charge Bleed-Off Tank, Valve, Measurement Section, and Isolators**

The tank is fabricated from a 12-inch, 20 gage, carbon steel pipe section that is approximately 21' long. Reducers (12x6) are welded to each end of the pipe. One end has a 6" single groove fitting and the other is a 6"-150 lb flange. The flanged end provides one side for a wafer style butterfly valve. On the other side of the butterfly valve, the electrical isolation spool is attached. The isolation spool is a 6" section of PVC pipe; approximately 9" long glued to 6" PVC flanges that fit the bolthole pattern of 6" ANSI flanges. All electrical isolators use this design. Of great practical advantage of the design shown in Figure 3 is that the tank centerline is low to the ground and therefore supporting connecting hose off the ground or leaving it on the ground is relatively easy and excessive bending moment stresses are not induced into the PVC isolators.

Figure 4 provides a photograph of an isolation section, coupled to a butterfly valve, and subsequently coupled to typical transition unit allowing the transition from an ANSI 6"-150 lb flange to the typical single groove Victaulic fittings used on IPDS components. Two transition items to convert from 6"-150 lb flange to 4" AHS were fabricated and used when installing the 4" hose. All items fabricated at SwRI were hydrostatically tested to ensure their structural integrity for the intended operating pressure of the flow loop.



**Figure 4. Photo of Butterfly Valve Connected to Isolator Section and Single Groove Transition.**

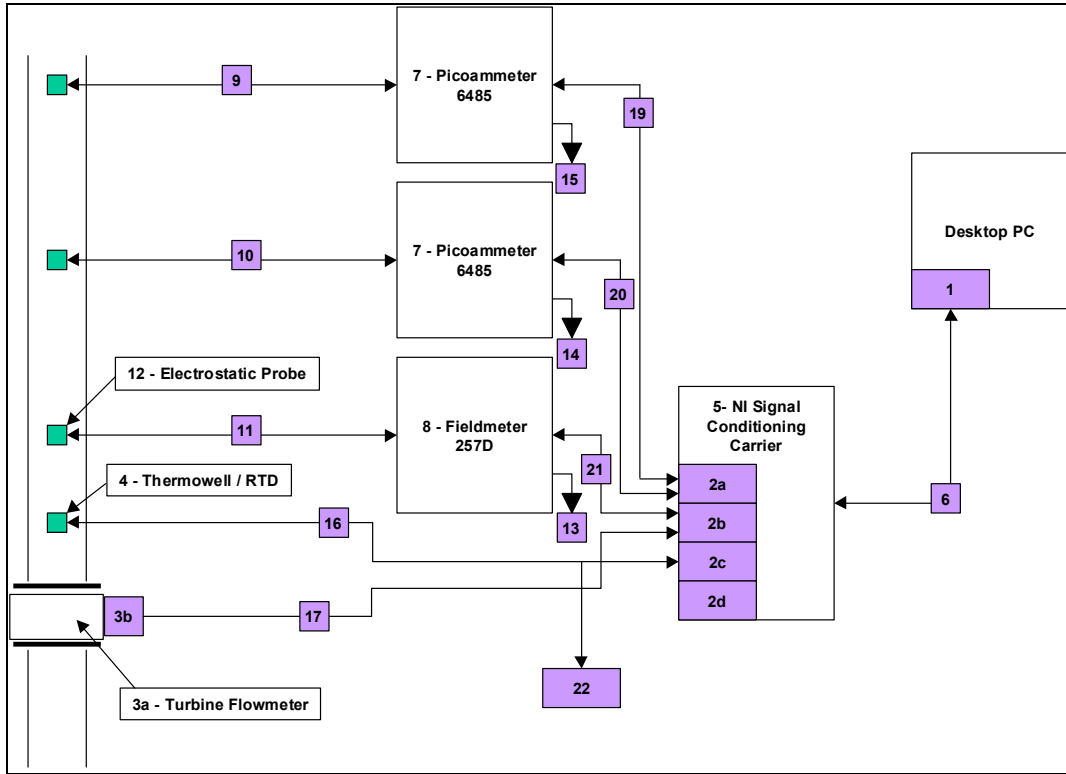
#### **3.2.2.4 Instrumentation and Data Acquisition**

Field-testing was conducted outdoors and therefore extra precautions were necessary to accommodate site limitations, weather conditions, and shipment and handling. Hence, an instrumentation cart was used as a platform for assembly all necessary instruments, computer (PC), and interfacing data acquisition equipment. This cart could be easily shipped along with critical instruments packaged separately. Once received on site, the assembly of the entire data acquisition system could be accomplished in about one hour. Also, the entire system could be put under cover in the event of rain or snow. Instruments mounted on the flow loop could also be covered to protect them from wet conditions.



**Figure 5. Photo of Instrumentation Cart**

Figure 5 provides a photograph of the instrument cart on site. This cart is complete with a power bus and all necessary terminal strips and associated connectors for rapid setup. The cart unit contains an electrostatic field readout, two picoampere meters, P/C unit, monitor, keyboard, mouse, and 16 channel A/D unit. Figure 6 presents a diagram of the instrumentation and data system including and interconnect diagram.



- 1 = NI-PCI-6220 (16 bit, 16 channel A/D)
- 2a = Analog Input Module                    SCC-AIO4 (±5V)
- 2b = Analog Input Module                    SCC-AIO4 (±5V)
- 2c = RTD Module                                SCC-RTD01 (RTD)
- 2d = Current Input                              SCC-CI20 (4-20mA)
- 3a = Turbine Flowmeter                      SP6-MB-PHL-V-4X
- 3b = Freq to DC converter                    SP711-3
- 4 = Thermowell / RTD                        Weed Instrument
- 5 = NI Signal Conditioning Carrier            SC-2345
- 6 = Shielded Cable, 68-pin
- 7 = Keithley Picoammeter                    Model 6485
- 8 = Monroe-Electronics                      Electrostatic Fieldmeter, Model 257D
- 9 = Picoammeter Cable:                      Instrument to Probe
- 10 = Picoammeter Cable:                     Instrument to Probe
- 11 = Fieldmeter Cable:                        Instrument to Probe (9 pin to 9 pin)
- 12 = Monroe-Electronics                      Electrostatic Probe, Model 1036F
- 13 = Fieldmeter Cable:                        Grounding cable
- 14 = Picoammeter Cable:                     Grounding cable
- 15 = Picoammeter Cable:                     Grounding cable
- 16 = RTD Cable:                                RTD to DAQ
- 17 = Flowmeter Cable:                        Amplifier to DAQ
- 18 = **N/A**
- 19 = Picoammeter Cable:                      Instrument to DAQ
- 20 = Picoammeter Cable:                      Instrument to DAQ
- 21 = Fieldmeter Cable:                        Instrument to DAQ
- 22 = Sensotec Readout

**Figure 6. Diagram Of Instrumentation and Data Acquisition System**

A brief description of streaming current and field measurements is provided below; however, a more detailed technical description and use of these specialized measurements are found in Section 6.0.

### 3.2.2.4.1 Streaming Current Measurement

The charge density in a hydrocarbon fuel flowing in either a plastic or metallic flow line may be determined by inserting a short length of electrically insulated metal pipe to form a 'measuring section' in which an isolated amount of relaxation current from the charged fuel may be conducted to ground for measurement.

The isolated six-foot length of IPDS pipe serves as the measuring section. Refer to Figure 3. A metal strap is connected to this section and fed into a very sensitive current meter know as a picoammeter because it can measure currents in the  $10^{-9}$  range. Considerable detail on streaming current measurement is presented in Section 6.0.



**Figure 7. Streaming Current Measurement Section**

Figure 7 illustrates one of two streaming current measurement sections installed in the loop at Fort Lee. The essential component of this measuring section is the larger diameter metallic pipe inserted in the flow line (top right) using electrically insulating couplings on each end (dark spool units). A sensitive ammeter is used to measure the relaxation current collected by this isolated section of pipe when charged fuel is present. The charge-collecting area of the inner surface, the flow rate through the section, and the sensitivity of the current measuring instrument govern the threshold level of charge measurable in the fuel.

Note: Materials described as plastic can refer to the hose liner, the entire hose, or a composite material consisting of through the weave extrusion of plastic like materials into a fiber mesh. The word plastic as used in this report is also applicable to hoses like the RIFTS hose, which has an extruded through the weave liner consisting of polyurethane material.

### 3.2.2.4.2 Electrostatic Field Strength Measurement

Electrostatic charge bound to the inner wall of a hose will exhibit a measurable static electric field in the space surrounding the hose. Specialized non-contacting instruments for measuring such static electric fields are available and are adaptable for field measurement on fuel hoses of interest.

The electrostatic field meter requires a special shielding arrangement made by encircling the hose with a metallic surface. In effect, this shield prevents extraneous fields from influencing the sensor and therefore the sensor sees only the field induced by the presence of the hose only. Figure 8 shows the shield used when testing 6" hose. The shield is approximately 2'-6" long, and the field sensor is supported by a bracket on the outside of the shield.

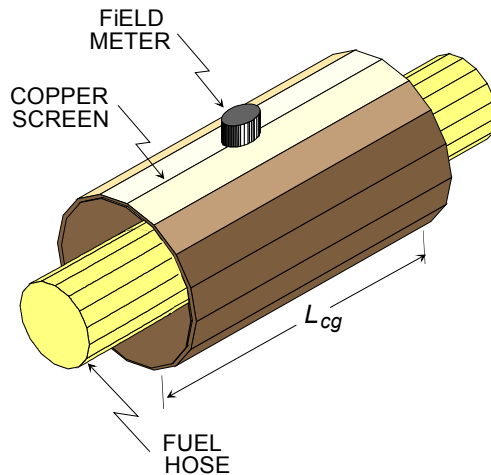


**Figure 8. Diagram of Electrostatic Field Sensor and Photographs of Shield System for 6-Inch Hose**

A calibration fixture composed of two parallel metal plates upon which a precise voltage is impressed is required to establish a field of known strength, typically of the order 10 kV/cm. The sensor to be calibrated is precisely positioned on one plate that is spaced at a known distance from the other parallel plate. Volts applied divided by the separation distance establishes the field strength.

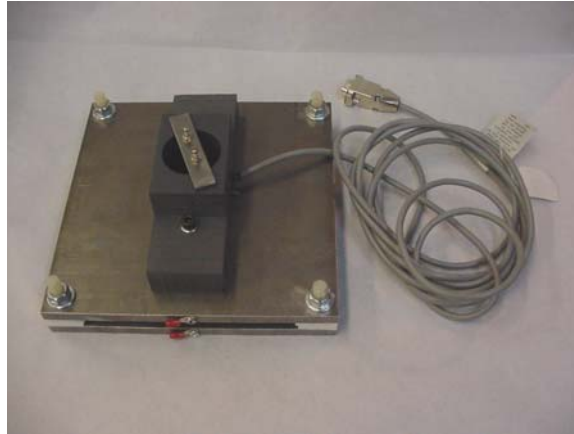


**Figure 9. Calibration Fixture - Field Sensor is Mounted in the Center.**

Large plates in comparison to the sensor aperture ensure that fringe effects are not influencing the sensor. Also, care is taken to round the edges of the plates to further reduce fringe effects at the edges. Insulators of precise thickness position the plates at a known separation and also provide electrical isolation of the plates. A photo of the field sensor installed on the calibration plates is shown in Figure 9. The general calibration procedure is to apply known voltages across the fixed gap plates and then plot the sensor output against these voltages. This results in a plot of sensor output versus field strength.

### **3.2.2.4.3 Measurement of Flow, Fuel Temperature, and Pressure**

An instrumented section of the loop just upstream of the first charge relaxation vessel contained a 6" Turbine flow meter with special single groove ends, an 18" long section with single groove ends with a pressure tap, and a 9" section with a special fitting to accommodate a thermowell for an RTD sensor. Certified calibration certificates were supplied with the turbine meter. The output from the turbine meter and RTD were fed into the data system and the output from the pressure transducer was fed into a Sensotec readout instrument (Model SC2000) and read off-line. It was necessary to ensure that the hose line had sufficient pressure to stiffen it up and take on a round shape. Normally, this occurs at pressures at 10 to 20 psi. (The AHS hose and the RIFTS hose operate at much higher pressure.) A photograph of the flow measurement section is shown in Figure 10.

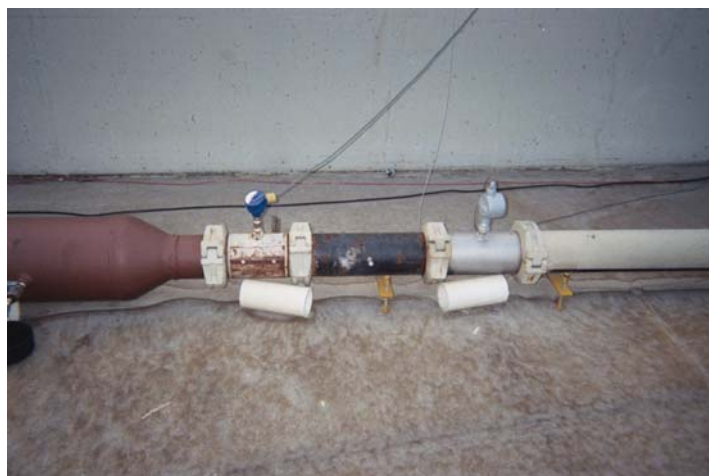


**Figure 10. Fuel Flow, Temperature, and Pressure Measurement Section**

### 3.2.2.4.4 Listing of Instruments

Instruments for both online and offline use plus other ancillary equipment required for the test program are provided in Table 1.

**Table 1. Test Variable and Quantification Method**

	<b>Test Variable</b>	<b>Range</b>	<b>Instrument Used/Comments</b>
1	Fluid Velocity	2.5 to >10.0 ft/s	6" Turbine Meter (200 to 2900 GPM range), Sponsler Model SP6-MB-PHL-V-4X, with SP711-3 frequency to DC converter
2	Hose ID	6.2"	Inflate and measure OD. Subtract 2x wall thickness
3	Length of test hose	500 ft	RIFTS hose in 500' lengths
4	Conductivity of Fuel	0 to 1999 pS/m	EMCEE Electronics, Model 1152 Conductivity probe, hand held, (ASTM D 2624), 3 – 6v Alkaline Batteries
5	Viscosity of Fuel	Typical of Jet A1	Compute using numerical model (need to know temperature)
6	Water content of Fuel	< 1%	ASTM method (collect samples)
7	Specific gravity of Fuel	Typical of Jet A1	ASTM method (collect samples)
8	Dielectric Constant of hose		Measured by ASTM method (sample taken from hose)
9	Streaming current	1 to 20 pa	Keithley Model 6485 Picoammeter, 2 channels required
10	Electrostatic Field Strength	20 kV/in	Monroe Electronics, Model 257 D Portable Electrostatic Field Meter
11	Temperature of Fuel	25 to 100 °F	Weed Instrument, Model 304, 100 Ω Platinum RTD,
12	Pressure of Fuel	50 to 150 psi	Sensotec Pressure Transducer, Super TJE , 1000 PSIA, accuracy of 0.05% full scale
13	Relative Humidity	1 to 99%	Amprobe, Model TH-2A, temp range –4 to 140 F, hand held, 3 AAA batteries required
15	Dimensional	Inch to Feet	Tape, Various items will require measurements of length

Components for the data acquisition system included:

- National Instruments, SCC Analog Input Module (Quantity of 2)
- National Instruments, SCC RTD Input Module
- National Instruments, SCC Current Input Module
- National Instruments, SC-2345 SCC Module Carrier
- National Instruments, NI-PCI-6220, M Series multifunction DAQ
- National Instruments, LabView Full Dev System for Windows
- Miscellaneous cables and connectors

#### **3.2.2.4.5 Installation of Test Loop at Fort Lee (December Tests)**

During the month of November, coordination of activities needed for successful installation of the test loop at Fort Lee were completed and test items and equipment developed by SwRI were shipped via a flatbed to Fort Lee on November 18, 2005. The shipment included two 500 ft long sections of RIFTS hose. Also as requested by Fort Lee, a complete test protocol including a safety and hazards assessment was sent to Fort Lee for review.

Assembly of the flow loop occurred over the period of November 29 through December 1, 2005. The arrangement of the equipment generally followed the layout plan with a few exceptions. This included the use of 6' long streaming current measurement sections in lieu of the planned 19' long sections. The physical layout of the 1000 ft of hose was also slightly altered. These changes were brought about to accommodate a slightly different arrangement of the 6" marine hose in the revetment (Tank 2) than anticipated. Also, a permanently installed electrical line running parallel to the 6" fill and drain line for the large 42' diameter tank consumed more floor space than anticipated.

Weather conditions were generally favorable during the installation, however rains were anticipated during the weekend of December 3 and 4. As such, the instrumentation cart was placed in a nearby heated building which had a floor space of about 10 ft by 10 ft. All other equipment was weather proofed either by covering equipment or placing the equipment in the shipping container. This proved to be a prudent move because heavy rains occurred starting December 4 and continued through December 5.

Photos of the installation with the RIFTS hose supported on electrical isolators are show in Figure 11. The temporary bridge between the two large revetments (tanks) is also shown.



**RIFTS 6" Hose Inside Tank 2**



**View of Field Measurement Device**



**Charge Relaxation Tank  
(upper right corner)**



**Bridge between Tank 1 and Tank 2**

**Figure 11. Photos of the Installation as Assembled for the December 2005 Tests**

### **3.2.3 Loop Configuration for August 2006 Tests**

During the tests in December 2005, the weather deteriorated, the necessary flow velocity for the 6" hose was not attainable, and measurements from the electrostatic field sensor were not fully understood. Hence, not all test objectives were obtained. Therefore follow on testing was recommended and this lead to the preparation for a new series of tests.

Three configuration changes were necessary; (1) modify the pump setup, (2) modify the streaming current calibration setup, and (3) concentrate on obtaining data for 500 feet of RIFTS hose only. The loop changes are highlighted in the following.

### **3.2.3.1 Pump Station Change**

The highest velocity obtained in the 6” hose in December was approximately 7.5 ft/sec, far below the required of at least 10 ft/sec. This necessitated changes in the pumping equipment; however, the inventory of available pumps with the desired pumping characteristics was limited, the 20K fuel bladder has only one 4” inlet and outlet, and there was limited suction hose and fittings. By clever arrangement of the available pumps, bladder, hoses, and a hose clamp, a pumping setup was devised that could not only provide the necessary 10 ft/sec, but also velocities in excess of 16 ft/sec were obtained. This pumping arrangement required careful “control” so that the net positive suction head requirements for each pump could be maintained. See Figure 13 for location of additional pump.

### **3.2.3.2 Additional Streaming Current Section**

To measure the amount of charge generated by the hose, it is necessary to obtain a measure of the amount of charge being generated by the measurement section itself and that of other parts of the loop. This accomplished by in effect removing the test hose and then measuring the streaming currents at the measurement sections (the 6 foot long sections of aluminum IPDS pipe). This may be accomplished by placing the measurement sections in tandem and then obtain streaming currents at various flow rates of fuel.

For the August test setup, it was determined that a clever way to accomplish this activity without the necessity of removing one measurement section and then placing it in tandem with the other is to place an identical section in tandem with one of the existing measuring sections. By inserting this section initially during the setup, then it is not necessary to drain fuel from the loop to make the move. This saves considerable time. See Figure 12 for a picture of the setup and Section 6.1.2 for details of the calibration process. See Figure 13 in the area marked “14.”



**Figure 12. Installation of Tandem Streaming Current Sections**

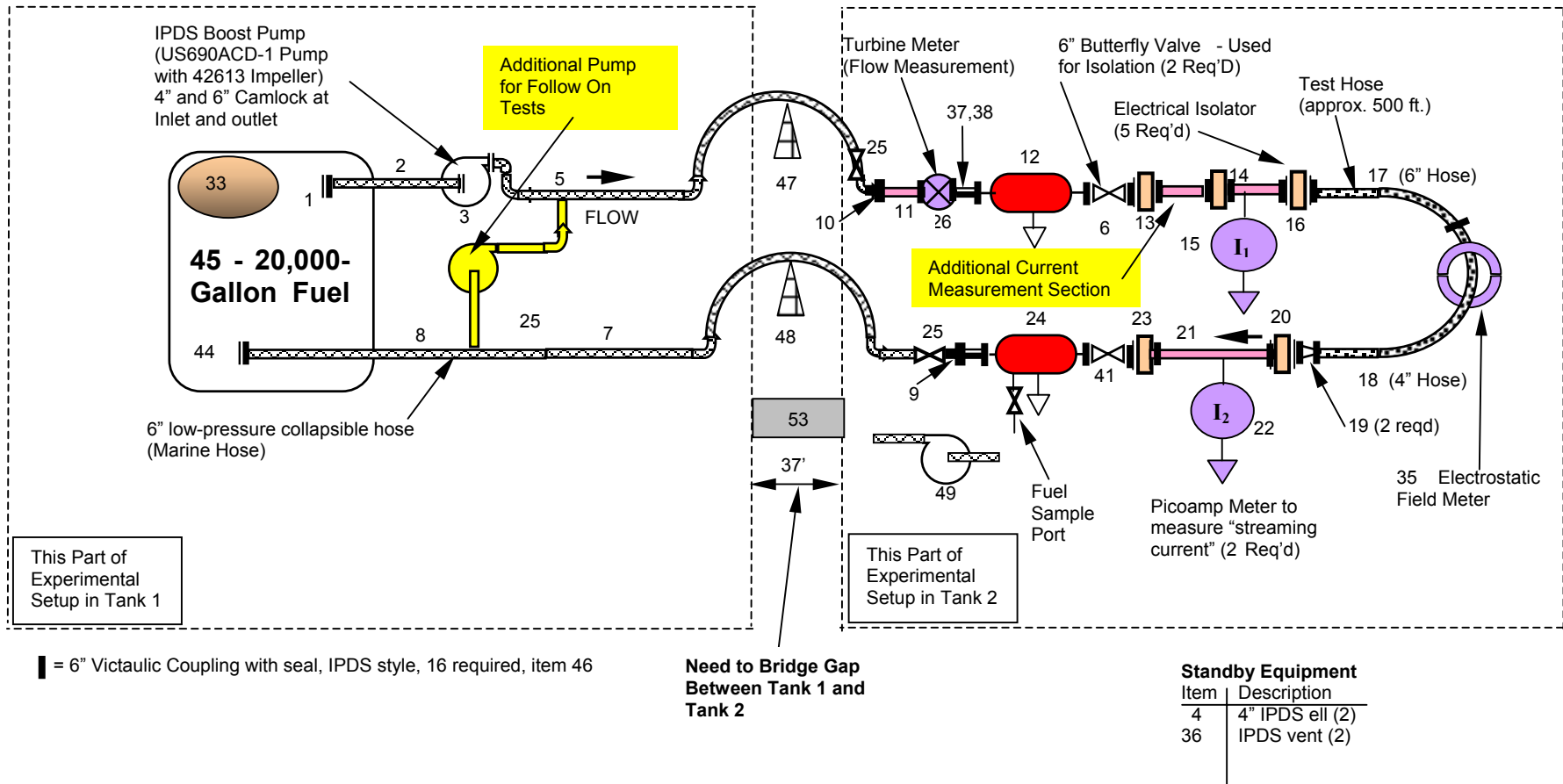


Figure 13. Loop Layout for August 2006 Tests

### 3.2.3.3 RIFTS Hose – 500 Feet

Based on the scientific data gathered during the December tests, it was found that surface voltages were well stabilized in the first 500 feet of hose and therefore, 1000 feet of hose is not needed for obtaining the electrostatic measurements. Also, during the December tests, the necessary fuel velocities in the 4" AHS hose were obtained, so priority was placed on obtaining data with 500 feet of the developmental RIFTS hose. Installation of 500 feet of hose is much easier to accomplish within the confines of the revetment and fewer turns are required for the hose. Fewer turns make the hose more similar to a long straight-line hose as would be expected under normal deployment conditions.

Shown in Figure 14 are several photos of the hose layout used in the August tests. Sections of deflated hose shown in the photos are sections of hose used in December that were not used for flow testing in August.



**Figure 14. Field Setup for August Tests Showing Bridge Between Tanks, Pump And Bladder Arrangement, and Views Of 6" RIFTS Hose On Electrical Isolators**

#### **4.0 Hose Configurations and Flow Conditions**

To investigate the need for a bond wire, it is desirable to test four configurations of the hose, which are (1) a hose with no bond wire while insulated from the ground, (2) a hose with no bond wire while the hose is in contact with the ground, (3) a hose with bond wire while supported above the ground, and (4) a hose with bond and in contact with the ground. Important test conditions needed are (1) a fuel with very low electrical conductivity, (2) fuel velocities in excess of those anticipated for intended field applications, (3) similar wall conditions of the hose of interest, which means the use of a replicate hose, and (4) reasonably close temperature conditions because of effects on boundary layer activity. Table 2 summarizes these configurations and conditions.

To generate the most charge possible and therefore the highest voltages, the test hose must be electrically isolated from any connecting hose or pipe and the test hose must not have a path to conduct current to ground. This is configuration 1 above. Electrical isolation is accomplished by using inline PVC spool isolators and by using 4" diameter PVC pipe sections to support the test hose. PVC is an excellent electrical insulator; however as will be discussed in following sections, current travels on the surface of insulators and therefore any dampness or conducting material collected on the surface can be cause for current drain off.

It was readily apparent during the initial phases of the test program that any contact of the unbonded hose and the ground would immediately drain charge and virtually mitigate any cause for concern regarding electrical hazards. In other words, the hose went to ground potential. Hoses lying on the ground went to ground potential. Therefore testing of configuration 1 under the required flow conditions will provide the necessary information to draw conclusions relative to the need for bonding and for determining if there is cause for concern regarding electrical breakdown.

Configurations and flow conditions for the December 2005 tests are very similar to those discussed above except the test matrix included 1000 feet of 4" AHS hose with and without bond wire, on and off the ground, resulting in four configurations. The test matrix also included the four configurations in Table 2 except the RIFTS hose was 1000 feet in length. Not all configurations were tested because the testing was cut short due to inclement weather and pumping problems as mentioned previously. However, test data was obtained for the most important and "worst case" configurations (hose without bond and supported off the ground) and these data are fully analyzed in Section 7.0.

**Table 2. Hose Configurations and Flow Conditions for August Tests**

<b>Config. No.</b>	<b>Configuration</b>	<b>Test Conditions</b>
1	<ul style="list-style-type: none"> <li>• Test with 500' of 6" RIFTS developmental hose that contains <b>no</b> static bond wire.</li> <li>• Hose supported off the ground with electrical isolators.</li> </ul>	Fluid Velocity Range: 2 to 10 ft/sec (min. of 4 velocity conditions) Fluid: Jet A1 Pressure: < 100 psi
2	<ul style="list-style-type: none"> <li>• Test with 500' of 6" RIFTS developmental hose that contains <b>no</b> static bond wire.</li> <li>• Hose in contact with ground.</li> </ul>	Fluid Velocity Range: 2 to 10 ft/sec (min. of 4 velocity conditions) Fluid: Jet A1 Pressure: < 100 psi
3	<ul style="list-style-type: none"> <li>• Test with 500' of 6" RIFTS developmental hose <b>with</b> simulated static bond wire.</li> <li>• Hose supported off the ground with electrical isolators.</li> </ul>	Fluid Velocity Range: 2 to 10 ft/sec (min. of 4 velocity conditions) Fluid: Jet A1 Pressure: < 100 psi
4	<ul style="list-style-type: none"> <li>• Test with 500' of 6" RIFTS developmental hose <b>with</b> simulated static bond wire.</li> <li>• Hose in contact with ground</li> </ul>	Fluid Velocity Range: 2 to 10 ft/sec (min. of 4 velocity conditions) Fluid: Jet A1 Pressure: < 100 psi

## 5.0 Electrostatics For Flexible Conduit

### 5.1 Flexible Fuel Hose Electrostatics Problem

Electrostatic charging of hydrocarbon fuels is known to occur in fuel transport pipelines, in fuel handling hoses, and in operational fuel supply lines. Charge buildup in flowing fuel is a result of triboelectric (frictional) charge separation in fuel molecules and impurities in the fuel during contact with the pipe wall. In field operations, charge can accumulate in storage tanks and, thereby, impose hazardous electrical energy concentrations sufficient to cause incendive arc discharges. This hazard problem, primarily associated with fuel transfer operations (tank-to-tank and tank-to-aircraft or vehicle), has been the principal impetus for reducing or controlling such fuel line electrostatic charging effects. In general, electrostatic charging in fuel lines and its related hazards are mitigated by the fact that all fuels are electrically conductive to some extent and, depending on the surface area of fuel contact and the pipe or hose material composition, the developed charge will decay with time to establish an equilibrium between the charging process and the charge decay process. Thus, safety considerations in fuel handling are achieved primarily by procedural techniques involving standardized methods for proper equipment grounding and for controlling fuel flow rates within limits known to be safe for each type of fuel transfer system.

In many fuel transport systems in which fuel flows continuously, even though electrostatic charge accumulation effects may not impose explosive hazards, the fuel charging and discharging processes are still active to cause flow-induced electrical currents onto and off of the fuel line components. Furthermore, the presence of electrical space charge within a non-

conducting fuel hose has an associated flow-related electrostatic potential that resides on the fuel column. This potential produces a corresponding static electric field surrounding the fuel hose. Of particular importance, the electrostatic potential will appear directly across the hose wall when the hose is laid in intimate contact with the ground. When the fuel flow rate is sufficiently high, the electrostatic potential across the hose wall can approach or exceed the dielectric strength of the hose material. Such high potentials pose a hazardous condition in which an electrical breakdown can occur through the hose wall, creating a fuel leakage pinhole and a carbonized path for successive high voltage breakdowns. This arc-through hazard in non-conducting fuel hoses is a well-known primary concern in regard to military and industrial fuel transfer systems. Specifically, any fuel leakage along a fuel transfer line and the potential for subsequent incendive arcing can cause fire damage and catastrophic disruption of fuel delivery.

The U.S. Army is presently developing a new and advanced flexible fuel hose and associated emplacement and retrieval systems for efficiently transferring fuels over extended arbitrary field routes. The new hose design is specified to have a lengthwise electrically conducting wire bonded on the external surface of the hose to ensure localized grounding when the wire is intentionally connected to earth ground. This grounding wire provides a self-contained grounding circuit that supplements the grounding contact between the hose and the ground on which it is laid. Because of the expense of manufacturing the new hose with the added grounding wire and the potential for wire breakage during the life of the hose, the practical necessity for such supplemental grounding has come into question. The present project efforts have been aimed at resolving this question through full-scale field tests on pre-production samples of the new hose.

## **5.2 Triboelectric Charging and Discharge of Dielectric Liquids in Pipe Flow**

### **5.2.1 Electrostatic Charging Phenomena**

Hydrocarbon fuel flowing in plastic or non-conducting hoses can produce electrostatic charging of the flow stream and establish a bound electrostatic charge on the inner wall of the hose. This effect is caused by friction-related triboelectric charge separation in the boundary layer of flow where long-chain fuel molecules tend to form a Helmholtz double layer of charge loosely bound to the inner surface. At sufficiently high flow rates, the charge on molecules polarized away from the inner wall may be stripped off by other moving molecules, leaving a static charge of opposite polarity more strongly bound by a stationary image charge at the hose wall interface. The charge accumulated by the moving molecules becomes mixed into the flow cross-section and is transported down stream potentially to be delivered to a fuel storage tank. This moving charge in the hose is designated as the fuel flow “streaming current”. Under steady flow conditions, the static charge on the inner wall of the hose remains fixed in place because of the high resistivity of the hose material. In general, a threshold level of flow velocity is required to initiate the charge separation process and there will be a difference in charge separation under laminar and turbulent flow because of differences in boundary layer flow versus velocity. More specifically, experimental evidence (Schön, 1965; Gibson, 1971) has shown that charge separation under laminar flow is approximately proportional to the flow velocity whereas, under

well developed turbulent flow, charge separation is approximately proportional to the square of flow velocity. However, in experimental tests performed by these and other researchers, the power-law exponent for turbulent flow implied above has only been bracketed within a range of about 1.5 to 2.2. Similar triboelectric charging effects also occur in metallic fuel pipes with the exception that the static charge at the inner pipe wall is readily conducted to ground, leaving only the mobile charge in the fuel stream. A state of equilibrium in the triboelectric charge generating process is established in sufficiently long hoses under steady-state fuel flow conditions. This equilibrium occurs when the electrostatic charge density in the boundary layer streaming current becomes sufficient to impose a repelling force on the polarized molecules bound to the inner wall of the hose and thereby prevent the kinetic frictional forces at the boundary from producing additional charge separation. Any change in the steady-state flow velocity will cause a readjustment in equilibrium between the electrostatic charge in the flow stream and that bound to the hose wall.

In addition to fuel flow velocity as a principal electrostatic charging parameter, many other physical factors are involved in the triboelectric charging process. These factors include the type of fuel and its electrical conductivity, the presence of suspended particulates, water content in the fuel, the surface roughness of the hose wall, the electrical resistivity of the hose material, the presence of fuel filters, the fuel temperature, etc. Therefore, predicting electrostatic charging in flexible fuel hoses is imperfect because of the many variables involved. Nevertheless, for a given fuel hose type and field installation, the type of fuel and its electrical conductivity together with flow velocity are the primary factors affecting the development of the flow stream electrostatic charge. In particular, hydrocarbon fuels having a specific conductivity less than about 40-50 pS/m have a strong propensity for triboelectric charging under practical fuel flow conditions. As an example, Jet A1 diesel fuel typically has a conductivity as low as about 1-2 pS/m, or less, and may be considered to be the fuel most likely to generate high electrostatic charge at flow velocities of only a few meters per second. In comparison, JP-8 fuel contains an anti-static additive that increases its conductivity to values much greater than 50 pS/m (typically specified to be in the range of 150 to 450 pS/m), causing it to be a low-charging fuel at practical fuel transport flow velocities. The presence of water in the fuel has the effect of increasing the generation of electrostatic charge because fine water droplets, themselves, can undergo double-layer charge separation as a supplemental triboelectric effect and can carry a greater amount of charge than single ionized molecules. Water content of only a few percent can significantly enhance the electrostatic charge produced under any given fuel flow condition. The use of fuel filters in the hose line also increases triboelectric charge separation because of the large surface area presented by the filter element and the fact that most of the molecules in the flow cross-section may come in contact with the filter. The electrical polarity of the streaming charge and its counter charge bound to the inner wall of the hose is dependent on the chemical properties of the fuel and the plastic hose material. The same polarity will be generated in a given hose system when handling the same type and purity of fuel.

## 5.2.2 Charge Dissipation Phenomena

When electrostatic charge is generated in a plastic or polyurethane-lined fuel hose, an excess charge of one predominant polarity resides in the fuel flow cross-section and an opposing polarity charge resides on the inner hose wall. Electrostatic attraction forces act to bring these charges together to be neutralized but, because of much higher dynamic forces in the flow, only those charged molecules that enter the stagnant boundary layer will be neutralized by electrostatic attraction. Nevertheless, the moving charged molecules near the boundary layer will tend to migrate by electrical conduction through the fuel as they travel down stream where they eventually may be neutralized by bound charges on the inner hose wall. Obviously, under equilibrium conditions, each time such a neutralizing charge transfer occurs, there will be an equal probability that a nearby triboelectric charge separation event may also occur to restore the net equilibrium streaming current. Therefore, the quantitative bulk charge separation between the streaming current and the bound surface charge will only decrease when the flow velocity is reduced. This manner of charge neutralization indirectly explains why fuels having higher electrical conductivity tend to generate lower net charge separation at the boundary layer. Correspondingly, for fuel flow in grounded metallic pipes, there is a similar counter charge residing at the pipe wall that acts as a rapidly adaptable image of the charge in the flow stream. In this case, if the fuel is sufficiently conductive to give the streaming charged molecules practical electrical mobility and the metal pipe is long enough to allow those charged molecules enough time to migrate to the pipe boundary, any upstream charge flow entering the metal pipe will tend to be neutralized by conductive charge decay to ground. This dissipation process can be of practical use as discussed in the following.

By using a metallic pipe section of somewhat larger diameter than the plastic or non-conducting hose to be tested to minimize velocity-dependent charge generation replenishment of the streaming current, this method of charge removal can serve as a means for minimizing any input charge in a fuel flow stream that is to be used in assessing the charge generated in a downstream test hose. In other words, a charge buffer or relaxation of charge tank is formed. Furthermore, by coupling an insulated section of metal pipe from ground, the relaxation current from the fuel in the pipe can be conducted to ground through an ammeter for measurement as a means for estimating the streaming current in the fuel flow (see Figure 16).

An accumulated electrostatic charge in a lossy dielectric liquid contained in a grounded metallic pipe or tank obeys an exponential decay law governed by the relaxation time constant of the liquid. That is, for a fixed initial charge,  $q_o$ , the charge at any later time is expressed by

$$q(t) = q_o \exp\left(-\frac{t}{\tau_f}\right) \quad (1)$$

where:

- $\tau_f = \epsilon_r \epsilon_o / \sigma_f$  = relaxation time constant of the fuel (sec);
- $\epsilon_f$  = relative dielectric constant of the fuel (dimensionless);
- $\epsilon_o$  = permittivity of free space (8.854 pF/m); and
- $\sigma_f$  = specific conductivity of the fuel (pS/m).

Equation 1 can be used to design charge dissipation or bleed-off tanks. Figure 15 shows the relative charge decay,  $q(t)/q_o$ , versus time for fuels having  $\epsilon_f = 2.1$  and conductivity ranging from 10 pS/m to 50 pS/m. For example, if a charged fuel flows through a 150-gallon grounded metallic storage tank, the chart in Figure 15 may be used to determine the residence time required for the fuel to undergo a specified amount of charge decay from a given initial charge. Using the chart for Jet A1 fuel having a conductivity of 10 pS/m and carrying an initial charge,  $q_o$ , a time interval of 7.27 sec is required for the charge to decay to two percent of the initial charge. Therefore, a parcel of the fuel moving through the 150-gal tank must reside there for at least 7.27 sec (0.121 min.) in order to be 98 percent neutralized by charge conduction to the tank wall. In this example, the maximum allowable volumetric flow rate through the tank is therefore  $150/0.121 = 1,240$  gal/min. The shape of the 150-gal storage tank is important in that the fuel velocity at the tank walls must be relatively low in order to avoid triboelectric charging in the tank. That is, if the onset flow velocity for triboelectric charge separation is assumed to be 1 m/sec, then the 150 gal tank can be in the form of a cylindrical section of pipe having an ID of 12.87 in. and a length of 24.8 ft. to accommodate conductive dissipation of the charged fuel at a continuous throughput volume flow rate of 1,240 gal/min. Correspondingly, this “storage tank” section of grounded pipe could be made larger in diameter and shorter in length to accomplish the same charge relaxation result. At lower flow rates in this pipe section, the fuel residence time will be longer and, therefore, the degree of charge neutralization will be greater than 98 percent.

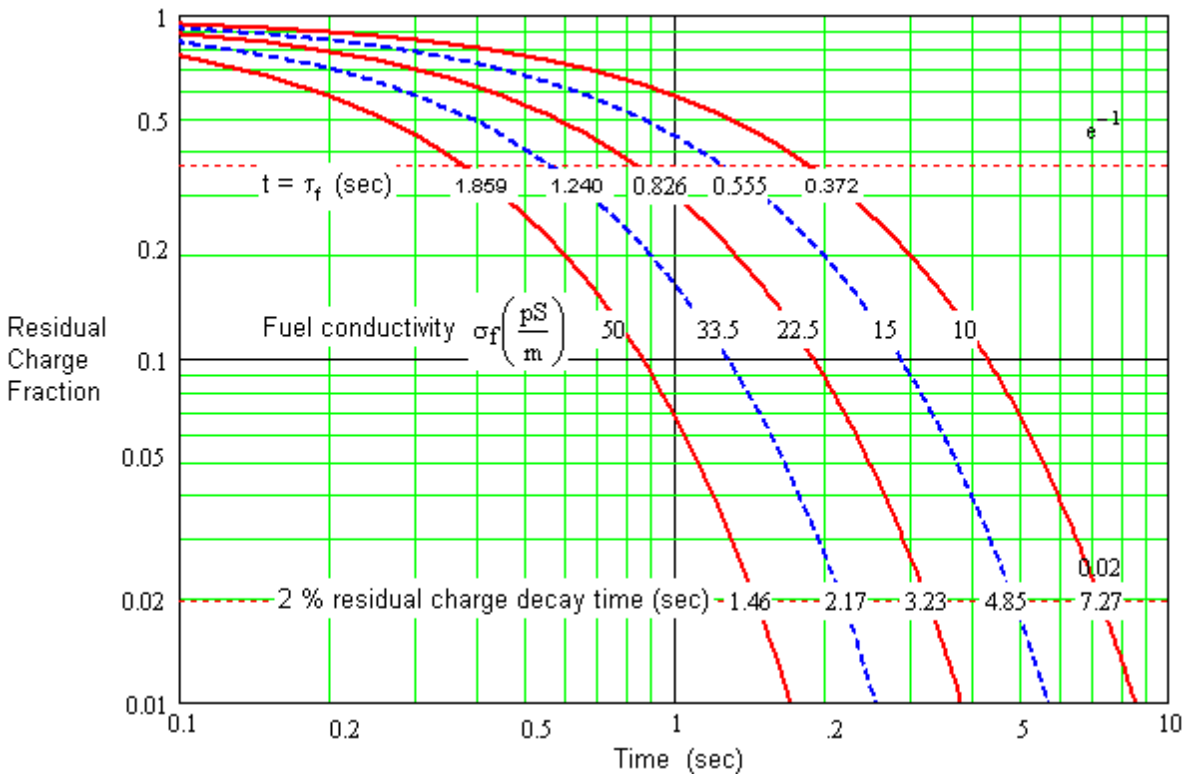


**Figure 15. Relative Charge Decay Versus Time for Hydrocarbon Fuels**

### **5.2.3 Electrostatic Hazards Related to Collapsible Fuel Hoses**

Hazards associated with hydrocarbon fuel flow in collapsible hoses are related to:

- (1) delivery of charged fuel to a destination fuel storage tank where it may accumulate and be slow to dissipate; and
- (2) high electrostatic potential across the hose wall caused by the presence of bound charge on the inner wall of the hose and the close proximity of sharp grounded objects at the outer surface of the hose.

#### **5.2.3.1 Charge Delivery**

As described above, a persistent electrostatic streaming current may be generated in plastic or non-conducting fuel hoses under equilibrium fuel flow conditions and is characterized by the movement of electrostatic charge through the hose at the fuel flow velocity. The magnitude of the streaming current is primarily dependent on the electrical conductivity of the fuel and the fuel flow velocity but is also influenced by a number of other factors that promote triboelectric charge separation at the inner wall of the hose. Safety guidelines at the fuel receiving location require that the charged fuel come in contact with grounded metal surfaces to promote charge dissipation. Grounded metal storage tanks and fuel tanker vehicles grounded to earth provide for such charge dissipation. Flexible bladder fuel storage tanks are similar to flexible fuel hoses in that the bladder presents a high electrical resistance to ground. However, the large surface area of such tanks in contact with the ground tends to facilitate dissipation of charge from the bulk volume of fuel. The use of metal piping at the receiving location provides additional grounding for dissipating charge in the fuel. The specific operational hazard concerning charged fuel in storage tanks is in handling grounded objects such as transfer hoses or piping at inlet or outlet connection points where incendive electrical sparks might occur in a local flammable vapor atmosphere.

#### **5.2.3.2 Electrostatic Potential**

The insulating properties of the plastic or non-conducting hose material impede the bound charge on the inner wall from being conducting to ground at external locations along the hose. With the exception of outer surface contamination effects, the internal volume of the plastic hose wall material is highly resistive. Typically, the volume resistivity of the plastic materials used in flexible hoses is on the order of  $10^{11}$  ohm-m and higher, depending upon the material. Therefore, considering the inner and outer hose surfaces as the plates of a charged capacitor, the charge relaxation time constant of the hose material will be on the same order of magnitude or higher than that of Jet A1 diesel fuel. The relative dielectric constant of the plastic material used in flexible hoses is in the range of about 2.5 to 4.5, depending upon the material. The electrical breakdown voltage (dielectric strength) of the plastic material used in flexible hoses is in the range of 300-500 kVDC/inch, depending on the materials and hose physical construction.

The intrinsic electrical properties of the plastic hose materials stated above are representative of very good insulators. However, in many cases, the hose is fabricated as a composite structure consisting of a woven fabric or polymer weave imbedded in the plastic for added tensile strength and pressure resistance. In practice, the cross-sectional area of the weave is approximately the same as that of the plastic binder material. Therefore, the electrical properties of the weave material contribute significantly to the effective electrical properties of the composite hose. Furthermore, since the weave may not be fully impregnated by the plastic binder, it will be porous and, therefore, lower in density and dielectric constant than the plastic material. Possible irregularities in the lay of the weave during fabrication can cause localized variations in the uniformity of the physical and electrical characteristics of the hose wall. Other fabrication defects such as inclusions, pinholes, and surface pitting also introduce local variations in hose electrical uniformity. In field applications, the plastic hose will undergo abrasion, outdoor exposure, and flexure in handling that could cause cuts, crimps, embrittlement, cracking of the plastic, and exposure of the web to moisture, all of which could affect the physical integrity and the electrical integrity of the hose.

The conditions that can affect the uniformity of the electric field between charge on the inner wall and counter charge on grounded surfaces or objects external to the wall of the hose are of interest in characterizing the electrical integrity of flexible plastic hoses. Under steady-state conditions, whenever there is a bound charge on the inner surface there will be an opposite-polarity image charge on the outer surface. In hoses made with internal web, there will be gradients in relative dielectric constant and the material with the lower dielectric permittivity will experience the highest electrical stress and a corresponding higher tendency for dielectric breakdown. Cracks, pitting, and pinholes in the outer surface will allow foreign material to migrate into the hose wall, causing sharp and possibly grounded intrusions that can concentrate the electric field and increase the probability of dielectric breakdown.

The specific operational hazard associated with non-uniform electric field concentrations is the tendency for electrical breakdown to occur through the hose wall. Such discharges can puncture the hose wall causing a fuel leak and lead to possibly subsequent arcing that could result in fuel ignition and fire at the leak. Another form of electric field concentration in the hose wall occurs when the hose is placed in contact with a grounded sharp metal object, such as the edge of an angle iron frame or similar structure. In this case, the localized ground contact will concentrate the electric field and potentially cause the local electrostatic surface charge density on the inner wall to increase, resulting in a further increase in the local electric field and possible breakdown of the dielectric hose material. The presence and quantitative magnitude of the static charge on the inner wall of the hose can be determined by means of non-contacting measurements of the associated electrical field external to the pipe when no grounded objects are in close local proximity to the hose. In particular, when such field measurements are performed under controlled test conditions, the electric field can be interpreted to indicate the electrostatic potential across the hose wall in the presence of an external grounded surface.

## 6.0 Measurement of Electrostatic Parameters

### 6.1 Measurement of Streaming Current in Flexible Fuel Hoses

#### 6.1.1 Theoretical Considerations

The charge density in a hydrocarbon fuel flowing in either a plastic, composite, or metallic flow line may be determined by inserting a short length of electrically insulated metal pipe to form a 'measuring section' in which an isolated amount of relaxation current from the charged fuel may be conducted to ground for measurement. This arrangement must be specialized for the desired measurements by making the diameter of the measuring section equal to or larger than that of the flow line to decrease the flow velocity and any associated triboelectric charging effects and to increase the residence time of a given parcel of fuel in the measuring section. That is, a larger cross-section of the measuring section will reduce the triboelectric separation currents flowing from the measuring section pipe to the fuel and will increase the residence time of the fuel in the measurement section.

Figure 16 illustrates the flow-line measurement section geometry. The essential component of this measuring section is the larger diameter metallic pipe inserted in the flow line using electrically insulating couplings on each end. A sensitive ammeter is used to measure the relaxation current collected by this isolated section of pipe when charged fuel is present in the enlarged section. The threshold level of charge measurable in the fuel is governed by the charge-collecting area of the inner surface, the flow rate through the section, and the sensitivity of the current measuring instrument.

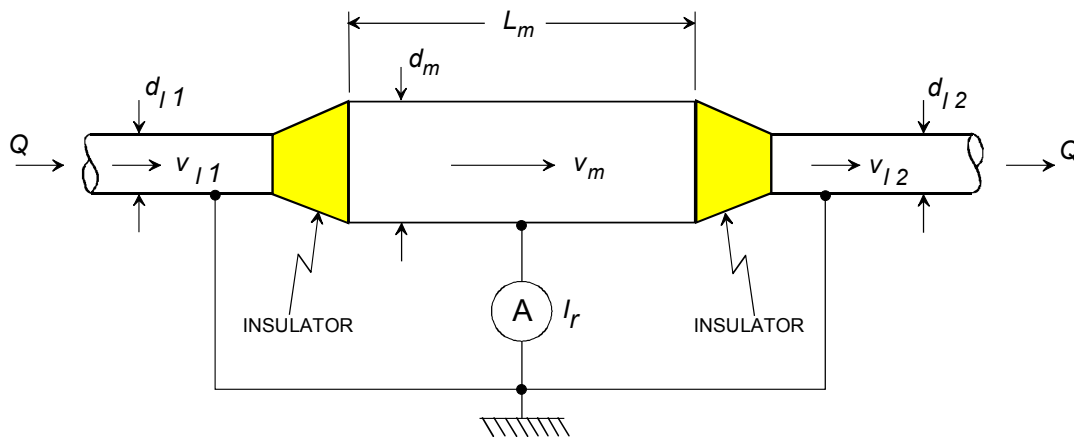


**Figure 16. Flow-Line Charge Measuring Section Geometry and Electrical Connections**

By quantifying the relaxation current measurement process via an analytical model representative of the triboelectric charging phenomena and fuel electrical properties, the measured current can be converted to a measure of the streaming current in the flow line and, hence, to a measure of the charge transported in the fuel flow. The experimentally derived

electrostatic charge transported in the flow represents the static electricity generated by the specific fuel flow line carrying a specific fuel composition and its dependence on the fuel volume flow rate. These relationships differ for laminar flow and turbulent flow conditions in the flow line. However, the fuel flow conditions in the military flexible hose fuel lines of interest in this study are generally always in the turbulent regime and, therefore, for evaluating high static charging effects, only the turbulent flow relationships are applicable.

The assumed model representing steady-state triboelectric streaming current (equilibrium charge transport) in a fuel flow line is, for turbulent flow conditions,

$$I_{\ell} = \rho_{TT} \cdot Q = B_{TT} \cdot \bar{v}_{\ell}^2 \quad (2)$$

and the associated streaming charge density in the turbulent fuel flow is

$$\rho_{TT} = B_{TT} \cdot \frac{\bar{v}_{\ell}}{A_{\ell}} \quad (3)$$

where:  $B_{TT}$  = triboelectric charging coefficient of the fuel and fuel flow line for turbulent flow conditions (coulAsec A m<sup>-2</sup>);

$$\bar{v}_{\ell} = \frac{Q}{A_{\ell}} = \text{mean flow velocity in the flow line (m/s);}$$

$$A_{\ell} = \text{cross-sectional area of the flow line (m}^2\text{);}$$

$$Q = \text{volume flow rate through the flow line (m}^3\text{/s);}$$

The fuel relaxation current produced by this streaming current when flowing through the electrically isolated metallic measuring section in the fuel line is

$$I_{rT} = \rho_{TT} \cdot Q \left( 1 - \exp\left(-\frac{t_m}{\tau_f}\right) \right) \quad (4)$$

where:  $t_m = \frac{L_m}{\bar{v}_m} = \text{volume flow transit time through the measuring section (sec);}$

$$L_m = \text{length of measuring section (m);}$$

$$\bar{v}_m = \text{mean flow velocity in the measuring section (m/sec);}$$

$$\tau_f = \frac{\epsilon_f \epsilon_o}{\sigma_f} = \text{fuel relaxation time constant (sec).}$$

$$\epsilon_f = \text{relative dielectric constant of the fuel (dimensionless);}$$

$$\sigma_f = \text{conductivity of fuel (Siemens/m);}$$

$$\epsilon_o = \text{permittivity of free space (8.854 pF/m);}$$

The relaxation current,  $I_{rT}$ , is an externally measurable parameter when the measuring section is insulated from the flow system ground. Other directly measurable parameters are the mean flow velocity,  $\bar{v}_m$ , (or volume flow rate,  $Q$ ) in the flow line and the fuel electrical properties,  $\sigma_f$  and  $\epsilon_f$ , which require separate off-line laboratory tests on the fuel. Thus, when these parameters are known from experimental measurements, the streaming current,  $I_P$ , entering the measuring section may be derived from

$$I_\ell = \frac{I_{rT}}{1 - \exp\left(-\frac{t_m}{\tau_f}\right)} \quad (5)$$

and, from Equation (2) and (5), the triboelectric coefficient of the combined fuel and flow line system is

$$B_{TT} = \frac{I_{rT} \cdot A_\ell^2}{Q^2 \left(1 - \exp\left(-\frac{t_m}{\tau_f}\right)\right)} \quad (6)$$

The dimensions and measurable parameters of the system shown in Figure 16 are:

$$v_\ell = \frac{Q}{A_\ell} = \text{mean flow velocity in the upstream flow line (m/s);}$$

$Q$  = volume flow rate through the flow line (m<sup>3</sup>/s);

$A_\ell$  = cross-sectional area of the flow line (m<sup>2</sup>);

$L_m, d_m$  = length and diameter of measuring section (m);

$d_{P1}, d_{P2}$  = diameter of flow lines upstream and downstream of measuring section (m).

The volume flow transit time through the measuring section is

$$t_m = \frac{\frac{\pi}{4} d_m^2 L_m}{Q} = \frac{L_m}{\bar{v}_m} \quad (7)$$

### 6.1.2 Flow Loop Checkout and Calibration

When two separately insulated measuring sections are connected in cascade in the flow loop, the upstream unit (measuring section #1) serves as a measurement reference for the downstream unit (measuring section #2). The ratio of the two experimentally measured relaxation currents provides a basis for determining the residual electrostatic charge density generated by the

pumping system and other parts of the flow loop prior to entering the test hose. In the cascade testing arrangement, the charge density exiting measuring section #1 is

$$\rho_2 = \rho_1 \cdot \exp\left(-\frac{t_m}{\tau_f}\right) \quad (8)$$

as a result of relaxation charge decay in measuring section #1. Therefore, the ratio of the two measured currents is, for identical measuring sections,

$$\begin{aligned} \left. \frac{I_{r2}}{I_{r1}} \right]_{\text{cascade}} &= \frac{\rho_2 \cdot Q \left(1 - \exp\left(-\frac{t_m}{\tau_f}\right)\right)}{\rho_1 \cdot Q \left(1 - \exp\left(-\frac{t_m}{\tau_f}\right)\right)} \\ &= \frac{\rho_2}{\rho_1} = \exp\left(-\frac{t_m}{\tau_f}\right) = R_{21} \end{aligned} \quad (9)$$

where:  $\rho_1 = \rho_P$  = flow line charge density entering measuring section #1 (coul/m<sup>3</sup>);  
 $\rho_2$  = streaming charge density exiting measuring section #1 and entering measuring section #2 (coul/m<sup>3</sup>); and  
 $R_{21}$  = experimental calibration factor for the cascaded measuring sections.

The calibration factor indicated in Equation (9) is a generalized relationship that does not necessarily require that the measuring sections be large enough to fully neutralize all fuel parcels in the section before they exit. In practice,  $R_{21}$ , is a flow-dependent factor that must be derived experimentally for the range of volume flow rates that will be used in testing sections of fuel flow line. Furthermore, the use of this cascade measuring section technique requires that some amount of streaming current be present upstream of measuring section #1 (i.e.,  $|\rho_1| > 0$ ). The residual charge density entering flow loop is

$$\rho_i = \frac{I_{r1}}{Q \left(1 - \exp\left(-\frac{t_m}{\tau_f}\right)\right)} = \frac{I_{r1}}{Q(1 - R_{12})} \quad (10)$$

Two cascaded measuring sections are essential for accurately measuring the triboelectric charging in a test section of fuel flow line when the fuel entering measurement section #1 carries an initial charge density,  $\rho_P$ , and/or when the flow conditions in the measuring sections also contribute to the streaming current. On the other hand, when the incoming streaming current is neutralized by allowing the fuel to reside in a suitably large grounded buffer storage tank or to flow through a large-diameter upstream metallic pipe where it is fully neutralized, only the downstream measuring section is needed to evaluate the charging effects in the test section of the flow line. In this case, the calibration process is reduced to determining the self-charging effects in current,  $I_{r2CAL}$ , versus fuel flow rate in the measuring section by coupling the insulated measuring section directly to the buffer storage tank. This value of self-generating current, including its algebraic polarity, is then subtracted from the current readings recorded with the

test section flow line connected. Furthermore, if the downstream measuring section #2 is also large enough to fully neutralize the streaming current generated by the test section flow line, then the calibration process is eliminated entirely. In this case, the relaxation current,  $I_{r2}$ , is a direct measure of the steady-state streaming current generated by the flow test section.

### 6.1.3 Measurement and Analysis of Streaming Current

For a test setup employing a suitably large grounded buffer storage tank upstream of the hose test section, a first measuring section is installed at the outlet of the buffer storage tank (measuring section #1). The purpose of this measuring section is to measure and monitor the triboelectric self-charging effects in the measuring section and introduced into the upstream end of the test hose. The relaxation current at this upstream position will be related to the flow velocity in the measuring section pipe and to the geometrical characteristics of the combined measuring section pipe and its insulating end couplers at the outlet of the buffer storage tank and at the inlet of the test hose. Then, with an identical measuring section located at the downstream end of the hose test section, the relaxation current at this position will be the combined result of the triboelectric charging in the two measuring sections and in the test hose. Assuming that the upstream relaxation current is primarily associated with triboelectric charging in the measuring section and its isolator end fittings, the net relaxation current associated only with triboelectric charging in the hose test section is

$$I_{r\ell} = I_{r2} - 2I_{r1} \quad (11)$$

Therefore, the streaming current in the test hose is, from Equation (5),

$$I_{r\ell} = \frac{I_{r2} - 2I_{r1}}{1 - \exp\left(\frac{Lm_{eff}}{\bar{v}_m \cdot \tau_m}\right)} \quad (12)$$

where:  $Lm_{eff} = (D_{ms}/D_{iso})^2 \cdot L_{mp}$  is the effective flow length of the measuring section pipe (m);

The effective flow length of the measuring section must be used instead of the actual length when the cross-sectional area is different from that of the test hose to account for the differences in the flow velocities in the measuring pipe and the hose.

The streaming charge density generated in the test hose is,

$$\rho_{TT} = \frac{1}{Q} \left[ \frac{I_{r2} - 2I_{r1}}{1 - \exp\left(\frac{Lm_{eff}}{\bar{v}_m \cdot \tau_m}\right)} \right] \quad (13)$$

and the triboelectric charging coefficient of the test hose is

$$B_{TR} = \frac{A_\ell}{Q^3} \left[ \frac{I_{r2} - 2I_{r1}}{1 - \exp\left(\frac{Lm_{eff}}{\bar{v}_m \cdot \tau_m}\right)} \right] \quad (14)$$

The triboelectric charging coefficient is a measure of the charge generated in the hose under the prevailing experimental conditions of hose length, layout, fuel type and fuel flow conditions. An important use of this coefficient is in comparing test hoses having different physical properties such as their material composition, internal coating, internal surface roughness, etc., when operated in similar layouts and with the same fuels.

Figure 17 shows a generalized arrangement for measuring electrostatic charging effects in plastic fuel hoses under various experimental testing conditions. In this arrangement, the upstream measuring section #1, depending upon its fuel transit time, may either be used as an active part of the system or otherwise grounded to earth by switch S1. The downstream measuring section #2 always serves as an active part of the system.

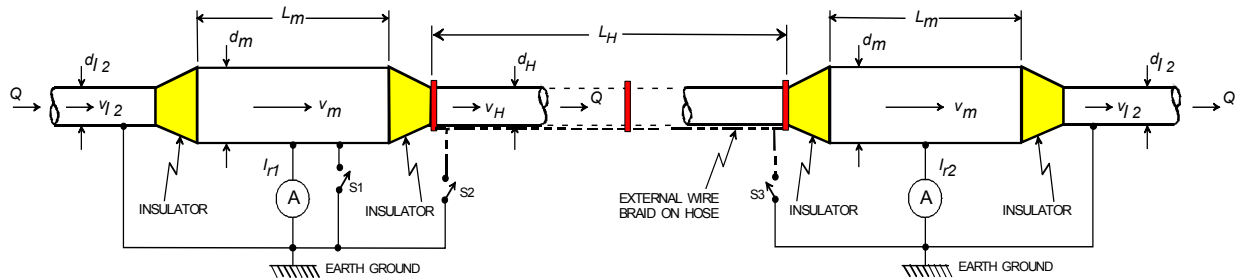


**Figure 17. Flow-Line Measuring Setup for Testing Fuel Hoses**

Fuel hose tests using this arrangement can accommodate a wide range of simulated field conditions, including:

- (1) Different types of fuels (Jet A1 fuel represents the fuel most sensitive to electrostatic charge generation);
- (2) Different fuel volume flow rates up to the maximum rating of the fuel hose to be tested;
- (3) Different types and sizes of fuel hoses, including hoses with and without integrally bonded grounding wire braid;
- (4) Different lengths of hose test sections;
- (5) Different earth grounding contact conditions along the hose test section, such as:
  - (i) Complete insulation from the ground;
  - (ii) Wire braid conductor along the hose section (if present) connected to ground at the upstream location, at the downstream location, or both;

- (iii) Simulation of a break in the wire braid at selected locations along the hose test section;
- (iv) External grounding wires installed at the intermediate hose couplings if the hose test section consists of multiple joints of hose;
- (v) Hose test section laid directly on the ground with and without the variations in wire braid and grounding options in (ii) – (iv) above and with water used to provide extremes in hose-to-ground contact.

## 6.2 Measurement of Electrostatic Potential on Flexible Fuel Hoses

Electrostatic charge bound to the inner wall of a plastic fuel hose will exhibit a measurable static electric field in the space surrounding the hose. Specialized non-contacting instruments for measuring such static electric fields are available and are adaptable for field measurement on plastic fuel hoses of interest. The static field around an isolated charged body is influenced by the proximity of nearby grounded objects and, in an associated way, by the size, shape, and electrical conductivity of the charged body. The electrical potential of the isolated charged body is related to its capacitance in relation to the ground and any nearby objects and to its stored electrostatic charge. The capacitance is determined by the size and shape of the isolated body and may be predicted analytically for simple geometrical configurations such as plane parallel plates, cylinders, and spheres. Otherwise, numerical solutions to Laplace's equation are required to establish the complicated charge distribution and electric potential associated with irregular shapes and surrounding ground surfaces. Nevertheless, for relatively simple geometrical shapes such as a wire of small radius, a cylinder of finite radius, a sphere, or a flat plate at or above a ground plane, the electric field distribution between the charged body and the ground may be accurately approximated and a measurement of the field, if made in a manner that does not distort the field distribution, can yield an estimate of the potential of the charged body.

To develop an understanding of such field measurements and interpreted electrical potentials, first consider the straight-forward case in which a non-contacting measurement of the electric potential of a metal plate is performed. This is a practical situation which is routinely used as a means of calibrating non-contacting field meters. In this case, the field meter is flush-mounted in the center of a metal plate, say, 2 feet in diameter, and grounded to earth. A second 2-ft diameter metal plate is connected to the positive terminal of a DC power supply at a voltage of, say, 500 VDC with the negative terminal of the power supply connected to earth ground. With the common ground connections and a fixed applied voltage between the plates, this arrangement is, in fact, a charged capacitor with air as the dielectric material between the plates. By locating the plates parallel and spaced at, say, 10 inches (0.254 m) apart, the electric field between them will be quite uniform in the center of the plates. The electric field is the potential gradient between the plates which, in this case, is constant at  $500\text{V}/0.254\text{ m} = 1968.5\text{ V/m}$ . The non-contacting field meter reading can be compared with this calculated value and its calibration adjusted to obtain accurate readings in any subsequent measurements. Furthermore, by orienting the field meter and its mounting plate normal to the charged plate at a spacing of 0.254 m, the measured field reading of 1968.5 V/m can be compensated for the spacing to yield the potential of the plate by multiplying the measured field by the plate spacing, i.e.,  $1968.5\text{V/m} \times 0.254\text{m} = 500\text{V}$ . In a practical outdoor measurement problem, the field meter and its baffle plate could be

mounted flush with the ground surface and a second plate of any size (typically larger) could be attached to the 500 VDC power supply and located parallel to the ground at a known height to provide an equally accurate determination of the potential applied to the plate. In this case, the size of the charged plate need not be known as long as it is large in comparison with the height above ground. Importantly, the potential of the plate is constrained to be constant and is unaffected by any nearby grounded objects. This elementary example is obviously clear and convincing when the power supply is connected to the elevated plate to establish the fixed applied potential.

The practical analog to this plane-parallel-plate example relevant to measuring the electrostatic potential on a cylindrical flexible fuel hose is one in which the grounded field sensor baffle plate is made cylindrical and oriented coaxially around the charged hose. With this arrangement, the image charge on the outer grounded metal cylinder, made of, say, copper screen or metal pipe, will exert a constant attractive force on the charge on the hose and, therefore, cause the surface charge density on both cylinders to become uniform and stable within a time period of about four times the relaxation time constant of the hose material. The electric field distribution and the capacitance of this coaxial cylinder geometry is readily calculated for the dimensions and plastic material involved and the electric field meter may also be flush-mounted in the outer grounded cylinder. The length of the outer cylinder should be about ten times larger than the annular air dielectric spacing between the inner cylinder and the outer cylinder. The electrostatic potential on the hose may be continuously monitored, if desired, to observe any changes in potential under different fuel flow rates or hose layout environmental conditions. The electrostatic shielding provided by the outer ground screen will also minimize the influence of any nearby grounded objects.

Figure 18 shows the coaxial cylinder arrangement for measuring the static electric potential of a plastic fuel hose. When the length,  $L_{cg}$ , is large compared with the annular spacing between the cylinders, the electric field within the annulus will only be dependent on the radial dimensions.

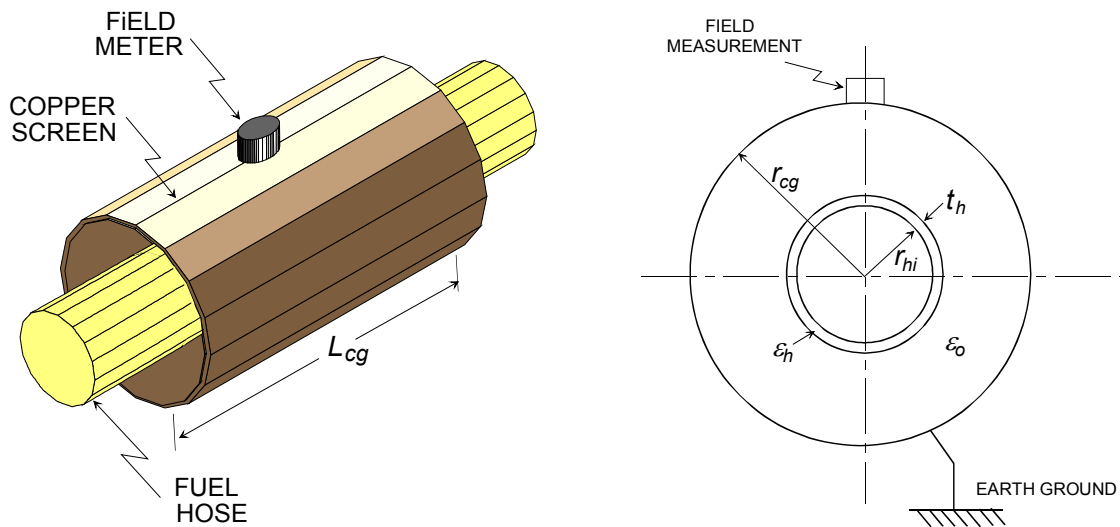


**Figure 18. Coaxial Fuel Hose and Surrounding Grounded Metallic Cylinder**

If the hose cylinder is assumed to have a uniform electrostatic charge per unit length,  $\sigma_h$ , on its inner surface, the surrounding electric field in the radial region,  $r_{hi} < r < r_{ho} = r_{hi} + t_h$ , will be

$$E_h = \frac{\sigma_h}{2\pi\epsilon_h\epsilon_o r} ; r_{hi} < r < r_{ho} \quad (15)$$

The maximum field value occurs at  $r = r_{hi}$  and decreases inversely with distance through the hose wall thickness. At the outer hose radius in the air annulus radial region,  $r_{ho} < r < r_{cg}$ , the electric field is

$$E_a = \frac{\sigma_h}{2\pi\epsilon_o r} ; r_{ho} < r < r_{cg} \quad (16)$$

In this region, the maximum field occurs at  $r = r_{ho}$  and decreases inversely with distance to  $r = r_{cg}$ . At the grounded outer cylinder, the measured electrical field is

$$E_{meas} = \frac{\sigma_h}{2\pi\epsilon_o r_{cg}} \quad (17)$$

Integrating this radially divergent field along the radial path from the inner wall of the hose to the grounded outer cylinder yields the electrostatic potential of the hose as

$$V_h = \frac{\sigma_h}{2\pi\epsilon_h\epsilon_o} \int_{r_{hi}}^{r_{ho}} \frac{1}{r} dr + \frac{\sigma_h}{2\pi\epsilon_o} \int_{r_{ho}}^{r_{cg}} \frac{1}{r} dr \quad (18)$$

For typical dimensions of the hose and grounded cylinder, say,  $r_{hi} = 3.0$  in.,  $r_{ho} = 3.35$  in., and  $\epsilon_h = 4.0$ , the potential difference across the hose material will be significantly smaller than the potential across the air annulus. Therefore, as a first approximation, the potential given by Equation (18) can be simplified and expressed, using Equation (17), as

$$V_{h1} \approx E_{meas} r_{cg} \ell n \left( \frac{2r_{cg}}{r_{hi} + r_{ho}} \right) \quad (19)$$

Furthermore, since the logarithmic factor is relatively small,

$$\ell n \left( \frac{2r_{cg}}{r_{hi} + r_{ho}} \right) = \ell n \left( \frac{9 \text{ in}}{3.175 \text{ in}} \right) = 1.042 \quad (20)$$

an additional approximation of the electrostatic potential of the hose is

$$V_h \approx E_{meas} r_{cg} \quad (21)$$

with an effective fractional error of only about -1.6 percent in comparison with the exact potential expressed by Equation (18). In effect, this approximation neglects the radial divergence of the electric field and treats the concentric cylinder system as an air-insulated parallel plate capacitor having a plate spacing of  $r_{cg}$ , where  $r_{cg}$  is the distance from the hose cylinder axis to the grounded outer cylinder.

The capacitance of the coaxial cylinder system, for the grounded cylinder length,  $L_{cg}$ , is

$$C_{coax} = \frac{2\pi\epsilon_o L_{cg}}{\frac{1}{\epsilon_h} \ln\left(\frac{r_{no}}{r_{hi}}\right) + \ln\left(\frac{r_{cg}}{r_{ho}}\right)} \quad (22)$$

which, for the typical dimensions stated above, may also be approximated by only the air annulus capacitance,

$$C_{coax} = \frac{2\pi\epsilon_o L_{cg}}{\ln\left(\frac{2r_{cg}}{r_{hi} + r_{ho}}\right)} \quad (23)$$

In terms of the capacitance of the coaxial cylinder measurement system, the potential and static charge on the hose are related by

$$V_{h\sigma} = \frac{\sigma_{hi} L_{cg}}{C_{coax}} \quad (24)$$

and the potential on the hose and the measured static electric field are related by

$$V_{hE} = \frac{2\pi\epsilon_o r_{cg} L_{cg}}{C_{coax}} E_{meas} \quad (25)$$

### 6.3 Fuel Hose Dielectric Breakdown

The dielectric strength of the hose is specified as the static electric field at which a potential difference across the hose wall thickness will initiate an electrical breakdown of the hose dielectric material. This electric field limit is typically in the range of 300 to 500 kV/inch in homogeneous polymer insulating materials, but may differ from this value in hoses having composite hose wall construction. For a hose inner radius,  $r_{hi} = 3.0$  in., a wall thickness,  $t_h = 0.35$  in., and a relative dielectric constant,  $\epsilon_h = 4.0$ , the typical static electric charge per unit length on the inner hose wall required to produce an electric field of  $E_{DS} = 400$  kV/inch (157.5 kV/cm) in the hose wall thickness is

$$\begin{aligned} \sigma_{hB} &= 2\pi\epsilon_h\epsilon_o(E_{DS}r_{hi}) \\ &= 2\pi(4)\left(\frac{8.854 \times 10^{-12}}{39.37}\right)(400 \times 10^3)(3.0) \\ &= 6.783 \mu\text{coul}/\text{inch} \quad (267.0 \mu\text{coul}/\text{m}) \end{aligned} \quad (26)$$

and the corresponding potential across the hose wall is

$$\begin{aligned}
 V_{hB} &= \frac{\sigma_{hB}}{2\pi\epsilon_h\epsilon_o} \ln\left(\frac{r_{ho}}{r_{hi}}\right) \\
 &= \frac{6.783 \times 10^{-6}}{2\pi(4)\left(\frac{8.854 \times 10^{-12}}{39.37}\right)} \ln\left(\frac{3.35}{3.0}\right) \\
 &= 132,420 \text{ volt}
 \end{aligned} \tag{27}$$

The corresponding electric field at the grounded cylinder of the coaxial system (i.e., the sensor-measured parameter) will be

$$\begin{aligned}
 E_{hB} &= \frac{V_{hB}}{r_{cg} \ln\left(\frac{r_{cg}}{r_{hi}}\right)} \\
 &= \frac{132,420}{9 \ln\left(\frac{9}{3}\right)} \\
 &= 13,390 \text{ volt/inch} \quad (5272.6 \text{ volt/cm})
 \end{aligned} \tag{28}$$

As a further simplification for interpreting the hose potential, the electric field measured at the grounded shield may be “scaled” to yield the approximate potential across the hose wall thickness by the relationship

$$\begin{aligned}
 V_{Bh} &\approx E_{hB} r_{cg} \ln\left(\frac{r_{ho}}{r_{ho} - t_h}\right) \\
 &\approx 13,390(9)\left(\frac{3.375}{3.0}\right) \\
 &\approx 134,595 \text{ volt} \quad (\text{within } 1.64 \% \text{ of } V_{hB})
 \end{aligned} \tag{29}$$

**Comment:** For composite flexible hose dielectric materials, the breakdown potential predicted above for homogeneous hose wall conditions will generally be reduced because of the inhomogenities in the hose composition. For example, since the AHS hose wall consists of a single polymer weave fully embedded in the extruded plastic wall material, the breakdown voltage predicted above may be a reasonably valid estimate (dielectric strength: 400 kV/in.). In comparison, the RIFTS hose wall is more inhomogeneous than the AHS hose wall because of its unbonded multiple layers of polymer fabric layers surrounding its inner elastomer liner. Therefore, the breakdown voltage of the RIFTS hose can be expected to be reduced significantly

from the idealized predicted value derived above. An estimated reduction factor in the range of about two to four (dielectric strength: 100 – 200 kV/in.) might be a realistic adjustment for the RIFTS hose taking into account the fact that the outer fabric layers may be penetrated by contaminating dust and moisture.

## **7.0 Fort Lee Field Tests**

A comprehensive analysis of data and field observations obtained from the Fort Lee tests is presented in this section.

### **7.1 Experimental Field Test Data and Analysis**

Field tests were performed at Fort Lee, VA in December 2005 and in August 2006. The first series of tests (Dec. 2005) was hampered by limitations associated with the fuel pump and flow loop setup as well as by inclement weather. In these tests, the pumping system could not maintain its fuel input prime at volumetric flow rates above about 900 gpm in the 1,000-ft test lengths of 6-in. diameter RIFTS hose and 4-in. diameter AHS hose. Maximum fuel flow velocities of 7.5 ft/sec for the RIFTS hose and 10.3 ft/sec for the AHS hose were insufficient to test the hoses at their normal or somewhat higher performance limits to evaluate their worst-case electrostatic characteristics. Inclement weather, with rain and icing, kept the test hoses wet much of the time, making any measurements of the hose electrostatic potential unreliable and generally much lower than anticipated from preliminary estimates. However, since the streaming currents within the hoses are not affected by the external hose environment provided that the measuring sections are dry and properly insulated, useful measurements of streaming currents were obtained for both hose types. Only the streaming current data for the two hose types tested in December 2005 are reported and analyzed below. The Jet A1 diesel fuel used in this first series of tests had an electrical conductivity of 1.5 pS/m.

The second series of tests (Aug. 2006) employed a modified pumping arrangement involving a second pump as a means of delivering input fuel from the downstream end of the loop directly to the input side of the main flow-loop pump. This powered partial bypass of the fuel storage bladder provided adequate input prime to the main pump to produce volumetric flow rates in the test hose as high as 1500 gpm. The scope of work planned for this series of tests involved evaluating only the 6-in. diameter RIFTS hose. The length of the test hose was reduced from the previous 1,000 ft. loop to 500 ft. length primarily to remove sharp bends and possible hose crimping when the hose was laid out in the confining concrete revetment at the test site. Inclement weather, with rain and high humidity, interfered with the planned tests, allowing productive streaming current measurements on only two days and productive hose potential measurements on only one of those days following the first field day devoted to fuel flow control adjustments and system checkout. The same Jet A1 fuel used in the first series of tests was stored on site and used again in the second series of tests. During the seven-month storage time, the electrical conductivity of the fuel increased from 1.5 pS/m to 22 pS/m.

## 7.1.1 December 2005 Field Tests

### 7.1.1.1 Streaming Current Measurements in the RIFTS Fuel Hose

Although several fuel flow tests were performed during the RIFTS hose experiments, the streaming current results of two representative tests are reported - the first with the hose laid on the floor of the concrete revetment (grounded condition) and the second with the hose supported on PVC isolators (insulated condition). In both tests the flow velocity was systematically increased from pump idle speed (mean flow rate approx. 2 ft/sec) up to the maximum available pump flow (mean flow rate approx. 9 ft/sec). Tests were also run with the flow decreasing from maximum to minimum with essentially the same streaming current results. The following RIFTS hose dimensions and fuel parameters were used in computing and analyzing the streaming current data:

RIFTS hose diameter:	$D_{RIFTS} = 6.20$ in.
Hose wall thickness:	$w_{RIFTS} = 0.35$ in.
Hose length (2 joints):	$L_{RIFTS} = 990$ ft.
Fuel electrical conductivity:	$\sigma_f = 1.5$ pS/m
Fuel relative dielectric constant:	$\epsilon_f = 2.1$
Permittivity of free space:	$\epsilon_o = 8.854$ pF/m
Fuel relaxation time constant:	$\tau_f = (\epsilon_f \cdot \epsilon_o) / \sigma_f = 12.4$ sec

Streaming current measuring section and associated flanged PVC isolator dimensions:

Measuring pipe diameter (ID):	$D_{ms} = 5.73$ in.
Measuring pipe inlet diameter (ID):	$D_{mi} = 6.20$ in.
Measuring pipe length:	$L_{mp} = 6.00$ ft.
Measuring pipe PVC isolator spool (ID):	$D_{iso} = 6.20$ in.
Measuring pipe effective flow length:	$L_{m_{eff}} = (D_{ms}/D_{RIFTS})^2 \cdot L_{mp} = 5.13$ ft.

Figure 19 and Figure 20 show the net measured relaxation current (picoammeter readings) versus fuel flow velocity before correcting for the effective flow length and the finite fuel residence time in the measuring section. With streaming current measuring sections installed at the upstream and downstream ends of the hose test section, the net relaxation current measured at the downstream section is the difference in magnitudes of the downstream current and twice the upstream current. The polarity of both currents was negative in all of the flexible hose flow loop tests. However, for clarity, Figure 19 and Figure 20 show the current magnitudes plotted as positive quantities. Figure 21 shows the Reynolds number versus fuel flow velocity for the Jet A1 fuel flow in the RIFTS hose, indicating that the transition from laminar flow to turbulent flow ( $Re \approx 2,000$ ) occurs at the lowest operating flow condition in the loop (pump idle speed: 800 rpm; fuel flow velocity: 2 ft/sec). The net relaxation currents range from about 7 nA to about 80 nA for both of the test runs. However, since the short measuring sections do not have a sufficient volume to allow all of the flowing charge to be measured before it exits the measuring section, the net relaxation current is corrected for the finite residence time required for a parcel

of fuel to traverse the effective flow length of the measuring pipe. The net streaming current in the test hose is, from Equation (12),

$$I_{\ell} = \frac{I_{r2} - 2I_{r1}}{1 - \exp\left(-\frac{Lm_{eff}}{\tau_f \cdot v_{\ell}}\right)} \quad (30)$$

where the smaller effective flow length of the measuring section is required to compensate for the difference in flow velocities in the measuring pipe and the hose, thereby allowing the measured flow-loop velocity to be used as a common factor in all expressions involving fuel flow.

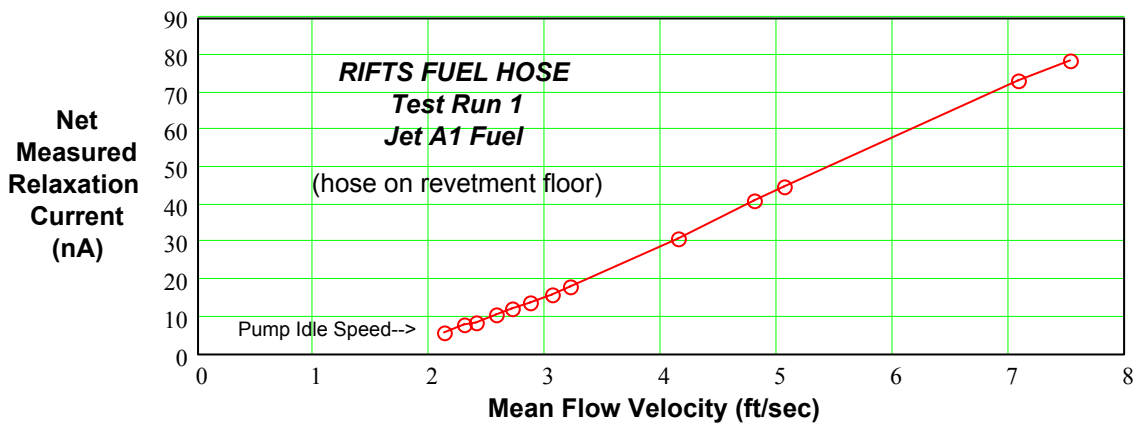


Figure 19. Net Relaxation Current in RIFTS Hose – Test Run 1 (Dec. 2005)

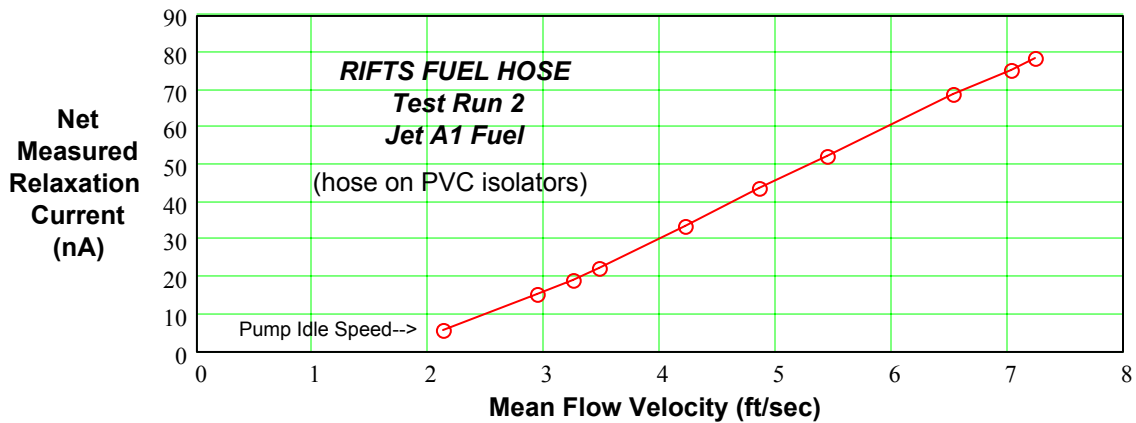
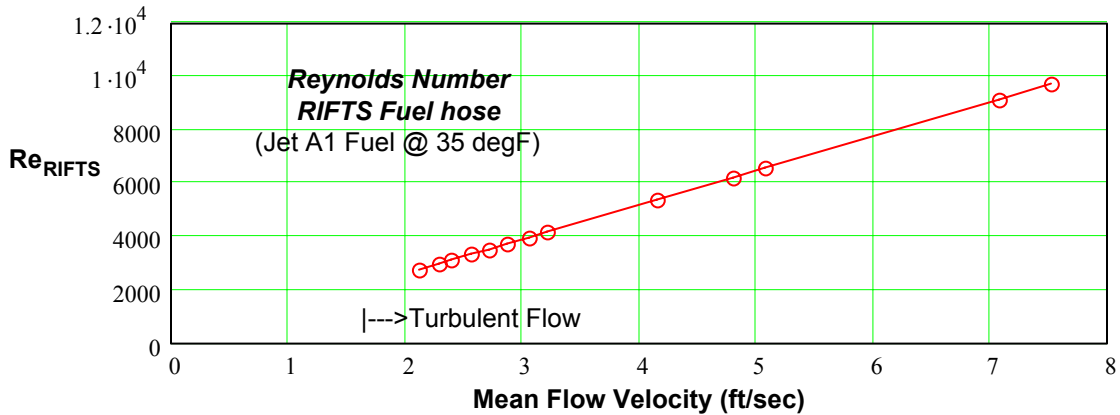
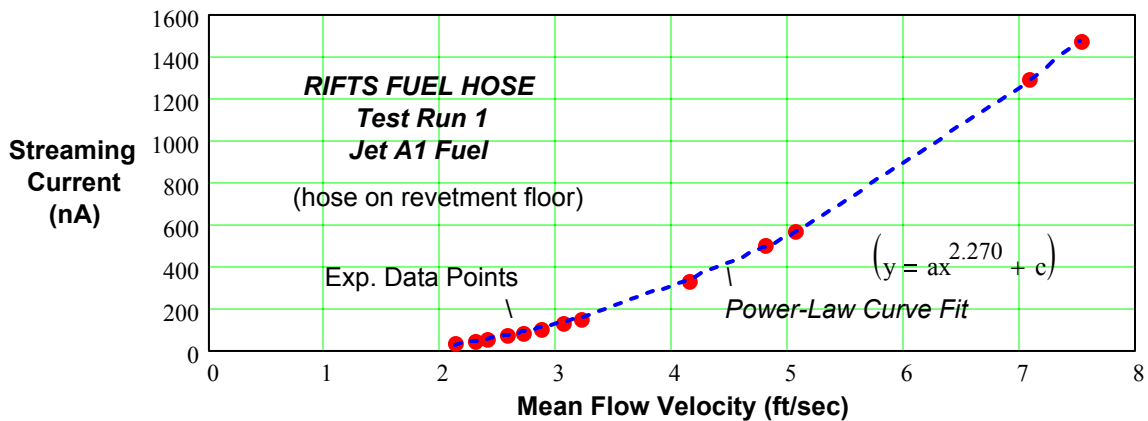


Figure 20. Net Relaxation Current in RIFTS Hose – Test Run 2 (Dec. 2005)



**Figure 21. Reynolds Number – RIFTS Hose, Jet A1 Fuel – (Dec. 2005)**

Figure 22 and Figure 23 show the corrected streaming currents together with least squares power-law curves fitted to the experimental data points. The fact that the functional dependence of streaming current on flow velocity differs for turbulent flow and for laminar flow (below about 2 ft/sec), the fitted curves have an offset relative to the  $v_f = 0$  origin. The best fit power-law exponent for the two test runs is in the range of 2.26-2.27; values that are acceptably close to the theoretical square-law dependence postulated in the earlier analysis.



**Figure 22. Streaming Current in RIFTS Fuel Hose – Test Run 1 (Dec. 2005)**

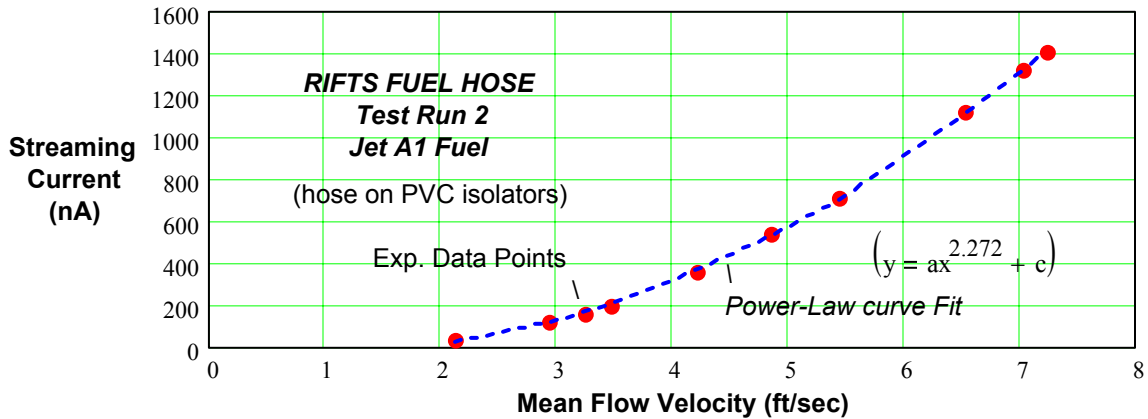


**Figure 23. Streaming Current in RIFTS Fuel Hose – Test Run 2 (Dec. 2005)**

Figure 24 presents the triboelectric charging coefficient,  $B_{TT}$ , for the RIFTS fuel hose. This coefficient, when fully developed for various experimental test conditions, can be a descriptive parameter that is useful for:

- (1) Predicting the streaming current in the RIFTS fuel hose from the fuel volumetric flow or fuel flow velocity;
- (2) A means for comparing production samples of RIFTS hose that incorporate different fabrication methods or materials; and
- (3) A reference parameter useful in research studies aimed at testing various hose fabrication materials, internal surface conditions, and static dissipater additives with the objective of quantifying and minimizing electrostatic charging in flexible fuel transport hoses.

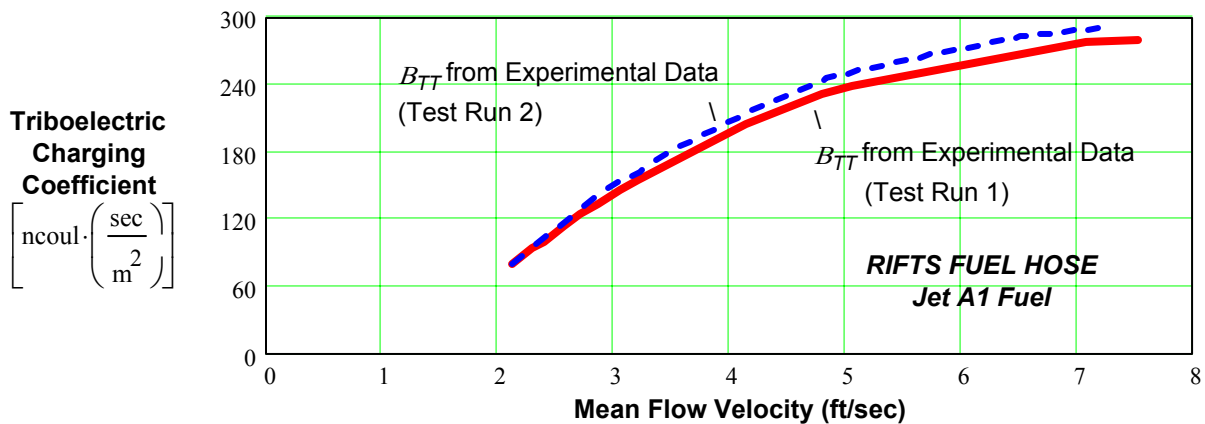


**Figure 24. Triboelectric Charging Coefficient – RIFTS Fuel Hose (Dec. 2005)**

### 7.1.1.2 Streaming Current Measurements in the AHS Fuel Hose

Several fuel flow tests were performed during the AHS hose experiments with the objective of determining the triboelectric streaming current and the hose potential when the hose was grounded and when the hose was supported on PVC isolators with the grounding wire on the outer surface of the hose grounded and ungrounded. Two representative tests showing the streaming current generated in the AHS hose are reported: The first with the hose laid on the floor of the concrete revetment (grounded condition with grounding wire connected to ground) and the second with the hose supported on PVC isolators (insulated condition with the grounding wire on the hose disconnected from earth ground). In both tests the flow velocity was systematically increased from pump idle speed (mean flow rate approx. 2.5 ft/sec) up to the maximum available pump flow (mean flow rate approx. 10 ft/sec). Tests were also run with the flow decreasing from maximum to minimum with essentially the same streaming current results. The following AHS hose dimensions and fuel parameters were used in computing and analyzing the streaming current data:

AHS hose diameter:	$D_{AHS} = 4.00$ in.
Hose wall thickness:	$w_{AHS} = 0.30$ in.
Hose length (2 joints):	$L_{AHS} = 980$ ft.
Fuel electrical conductivity:	$\sigma_f = 1.5$ pS/m
Fuel relative dielectric constant:	$\epsilon_f = 2.1$
Permittivity of free space:	$\epsilon_o = 8.854$ pF/m
Fuel relaxation time constant:	$\tau_f = (\epsilon_f \cdot \epsilon_o) / \sigma_f = 12.4$ sec

Streaming current measuring section and associated flanged PVC isolator dimensions:

Measuring pipe diameter (ID):	$D_{ms} = 5.73$ in.
Measuring pipe inlet diameter (ID):	$D_{mi} = 6.20$ in.
Measuring pipe length:	$L_{mp} = 6.00$ ft.
Measuring pipe PVC isolator spool (ID):	$D_{iso} = 6.20$ in.
Measuring pipe effective flow length:	$L_{m_{eff}} = (D_{ms}/D_{ahs})^2 \cdot L_{mp} = 12.31$ ft.

Figure 25 and Figure 26 show the net measured relaxation current (picoammeter readings) versus fuel flow velocity before correcting for the effective flow length and the finite fuel residence time in the measuring section. With streaming current measuring sections installed at the upstream and downstream ends of the hose test section, the net relaxation current measured at the downstream section is the difference in magnitudes of the downstream current and twice the upstream current. The polarity of both currents was negative in all of the flexible hose flow loop tests. However, for clarity, Figure 25 and Figure 26 show the current magnitudes plotted as positive quantities. Figure 27 shows the Reynolds number versus fuel flow velocity for the Jet A1 fuel flow in the AHS hose, indicating that the transition from laminar flow to turbulent flow ( $Re \approx 2,000$ ) occurs at the lowest operating flow condition in the loop (pump idle speed: 800 rpm; fuel flow velocity: 2.5 ft/sec). The net relaxation currents range from about 7 nA to about 50 nA for both of the test runs.

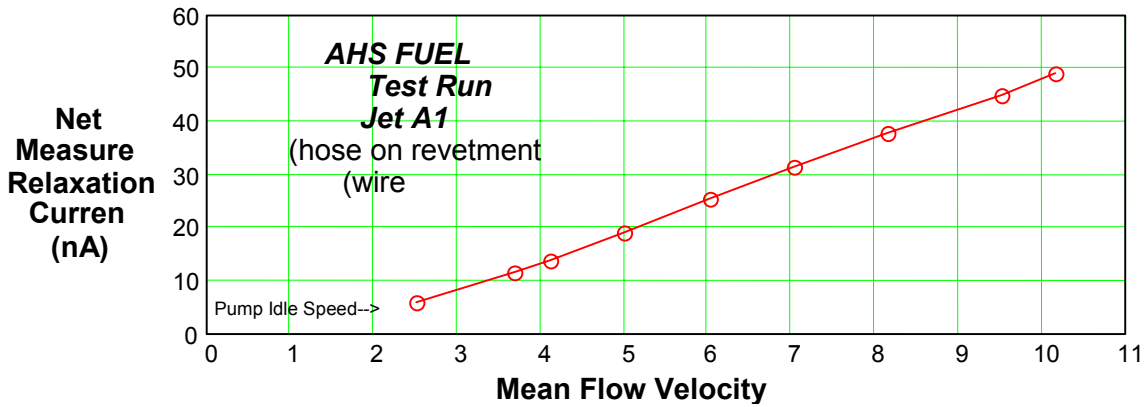


Figure 25. Net Relaxation Current in AHS Hose – Test Run 1 (Dec. 2005)

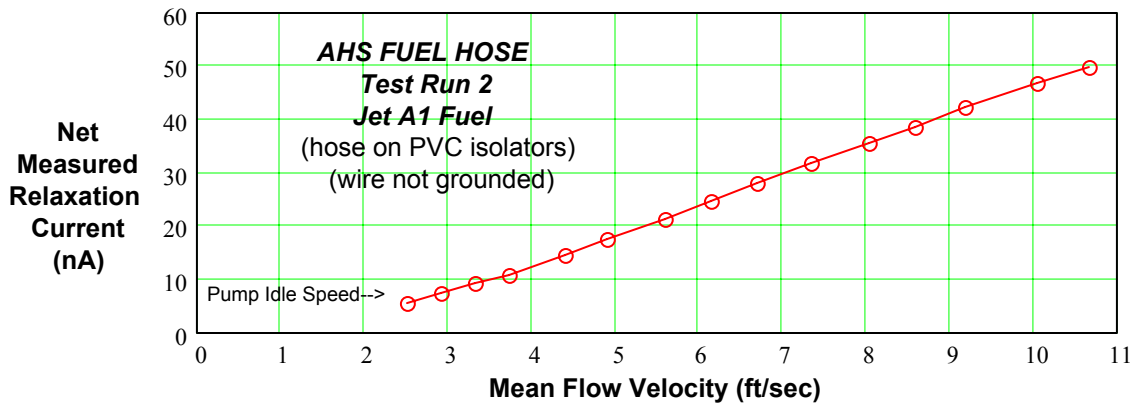


Figure 26. Net Relaxation Current in AHS Hose – Test Run 2 (Dec. 2005)

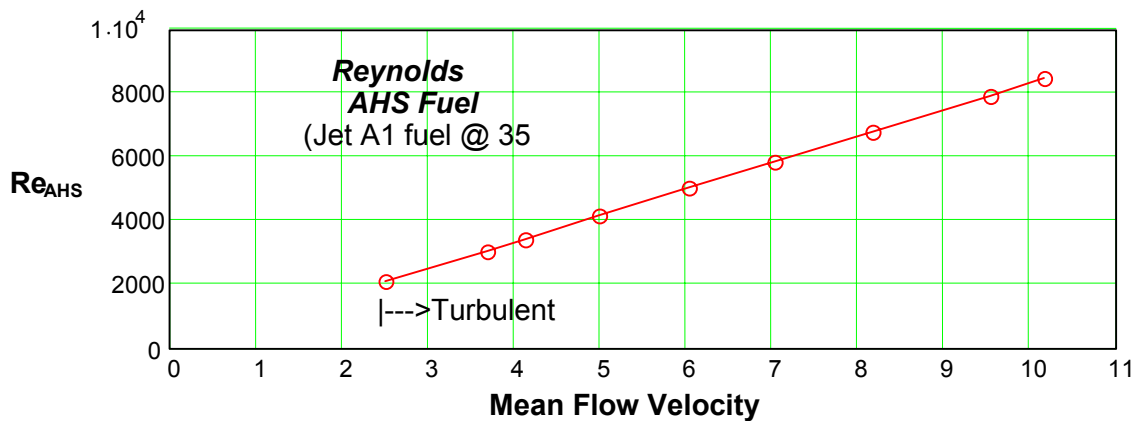


Figure 27. Reynolds Number – AHS Hose, Jet A1 Fuel – (Dec. 2005)

Figure 28 and Figure 29 show the corrected streaming currents together with least squares power-law curves fitted to the experimental data points. The fact that the functional dependence of streaming current on flow velocity differs for turbulent flow and for laminar flow (below about 2.5 ft/sec), the fitted curves have an offset relative to the  $v_f = 0$  origin. The best fit power-law exponent for the two test runs is in the range of 2.14-2.21; values that are acceptably close to the theoretical square-law dependence postulated in the earlier analysis.

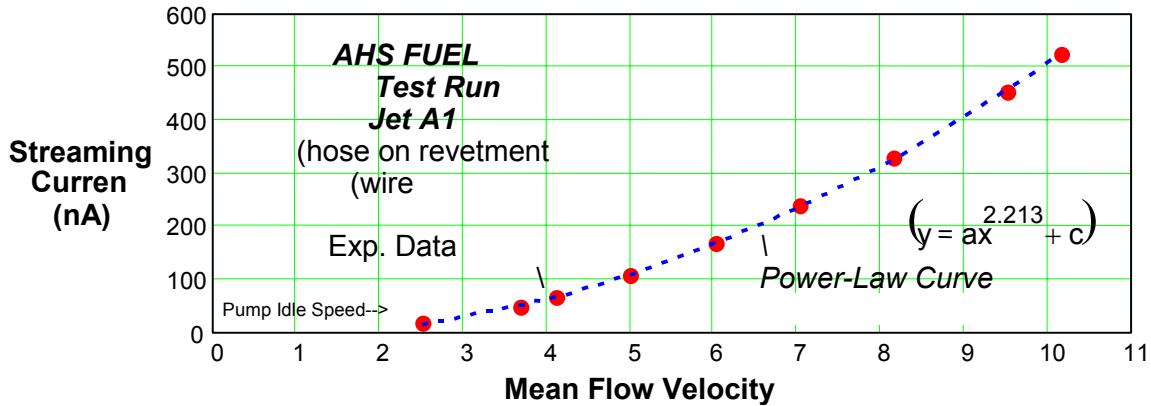


Figure 28. Streaming Current in AHS Fuel Hose – Test Run 1 (Dec. 2005)

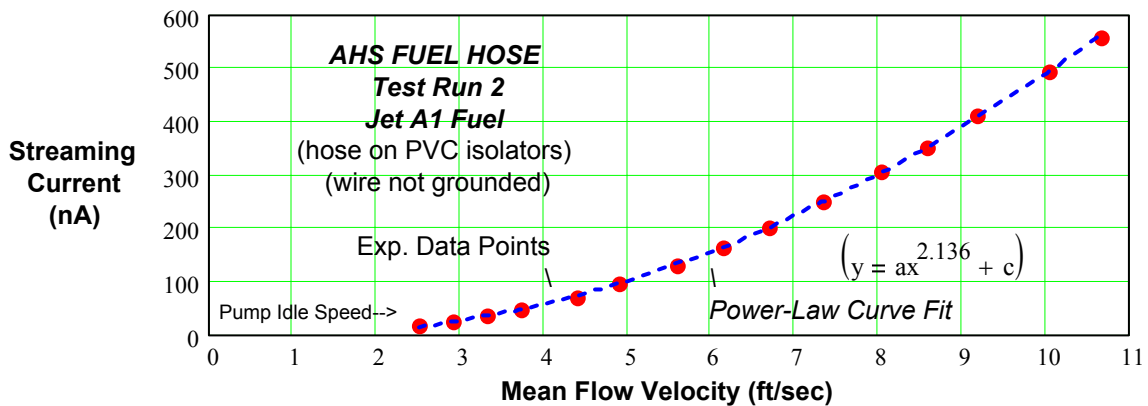


Figure 29. Streaming Current in AHS Fuel Hose – Test Run 2 (Dec. 2005)

Figure 30 presents the triboelectric charging coefficient,  $B_{TT}$ , for the AHS fuel hose.

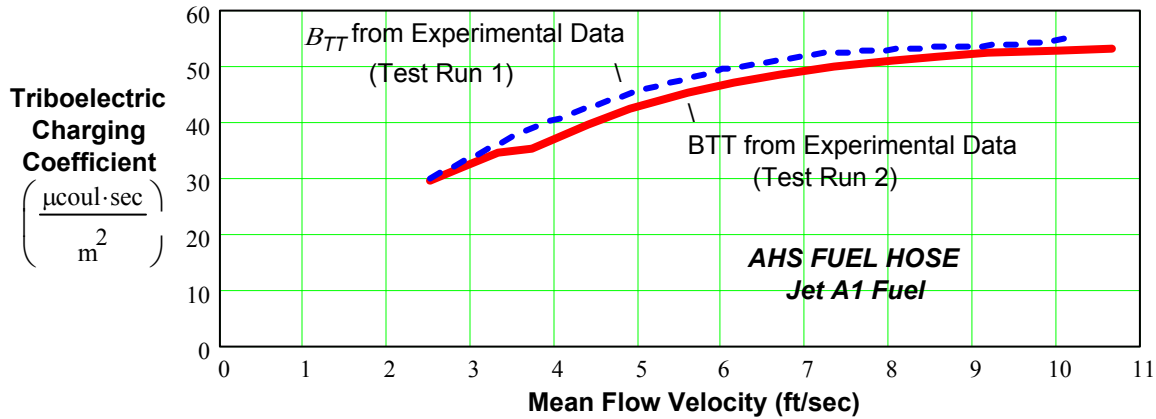


Figure 30. Triboelectric Charging Coefficient – AHS Fuel Hose (Dec. 2005)

## 7.1.2 August 2006 Field Tests

### 7.1.2.1 Streaming Current Measurements in the RIFTS Fuel Hose

Several fuel flow tests were performed using the higher fuel flow rates attainable in the August 2006 field tests of the RIFTS flexible fuel hose. Four representative tests are reported to illustrate the electrostatic streaming currents measured in the hose. Except for the use of only one joint of the RIFTS hose, the hose dimensions and streaming current measuring sections are the same as described for the December 2005 field tests. An important difference in the August 2006 tests and the December tests is in the Jet A1 fuel electrical conductivity. Because of the seven-month on-site fuel storage time, the conductivity increased from 1.5 pS/m to 22 pS/m. This change reduced the fuel relaxation time constant from 12.4 sec in the December 2005 tests to 0.845 sec in the August 2006 tests. The tested RIFTS hose length and the Jet A1 fuel electrical characteristics in the August 2006 field tests were:

Hose length (2 joints):	$L_{AHS} = 490$ ft.
Fuel electrical conductivity:	$\sigma_f = 22.0$ pS/m
Fuel relative dielectric constant:	$\epsilon_f = 2.1$
Permittivity of free space:	$\epsilon_o = 8.854$ pF/m
Fuel relaxation time constant:	$\tau_f = (\epsilon_f \cdot \epsilon_o) / \sigma_f = 0.845$ sec

Figure 31 through Figure 34 show the net measured relaxation current (picoammeter readings) versus fuel flow velocity before correcting for the effective flow length and the finite fuel residence time in the measuring section. With streaming current measuring sections installed at the upstream and downstream ends of the hose test section, the net relaxation current measured at the downstream section is the difference in magnitudes of the downstream current and twice the upstream current. The polarity of both currents was negative in all of the flexible hose flow loop

tests. However, for clarity, Figure 31 through Figure 34 show the current magnitudes plotted as positive quantities. Figure 35 shows the Reynolds number versus fuel flow velocity for the Jet A1 fuel flow in the RIFTS hose, indicating that the transition from laminar flow to turbulent flow ( $Re \approx 2,000$ ) occurs at the lowest operating flow condition in the loop (pump idle speed: 800 rpm; fuel flow velocity: 2 ft/sec). The net relaxation currents range from about 7 nA to about 80 nA for both of the test runs. However, since the short measuring sections do not have a sufficient volume to allow all of the flowing charge to be measured before it exits the measuring section, the net relaxation current is corrected for the finite residence time required for a parcel of fuel to traverse the effective flow length of the measuring pipe. The net streaming current in the test hose is derived using Equation (12).

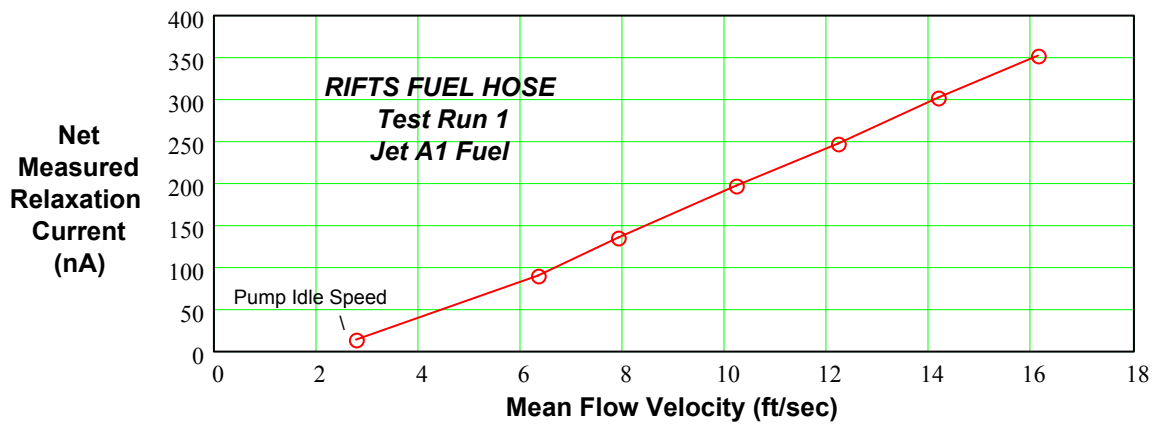


Figure 31. Net Relaxation Current in RIFTS Hose – Test Run 1 (Aug. 2006)

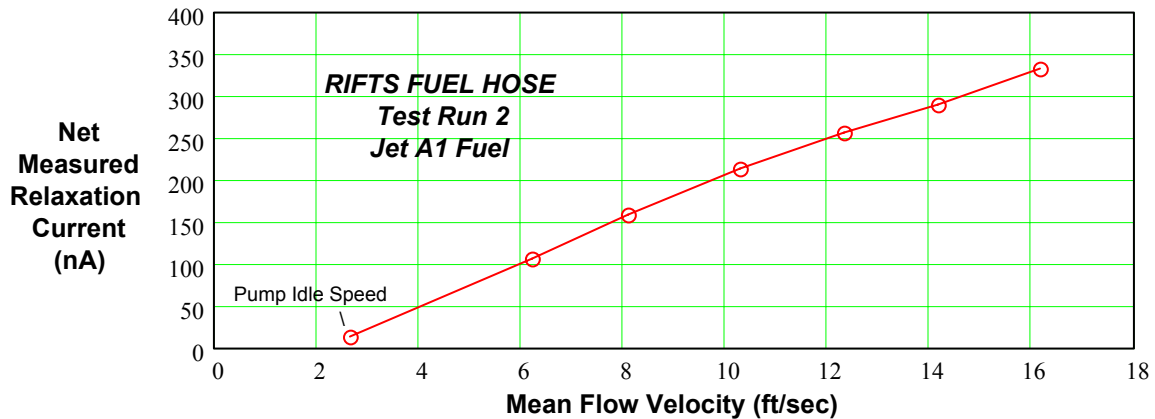


Figure 32. Net Relaxation Current in RIFTS Hose – Test Run 2 (Aug. 2006)

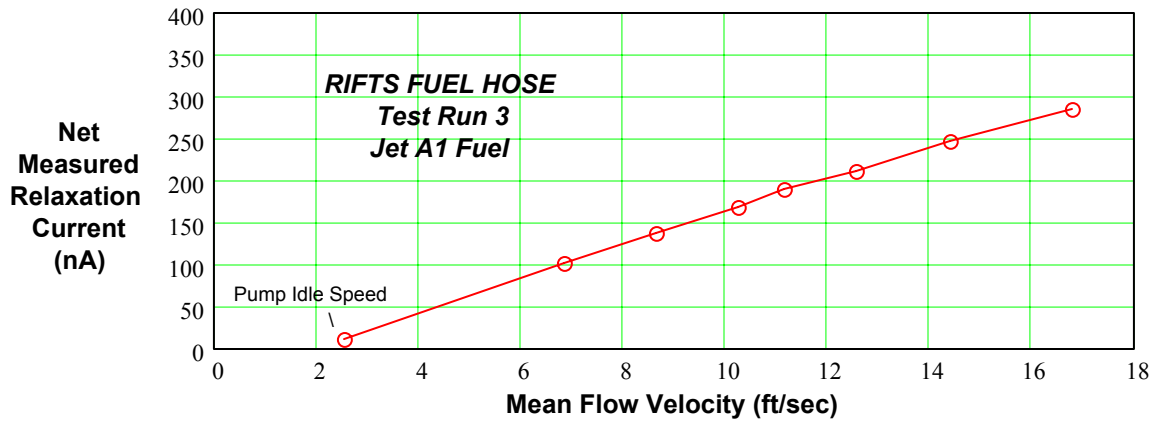


Figure 33. Net Relaxation Current in RIFTS Hose – Test Run 3 (Aug. 2006)

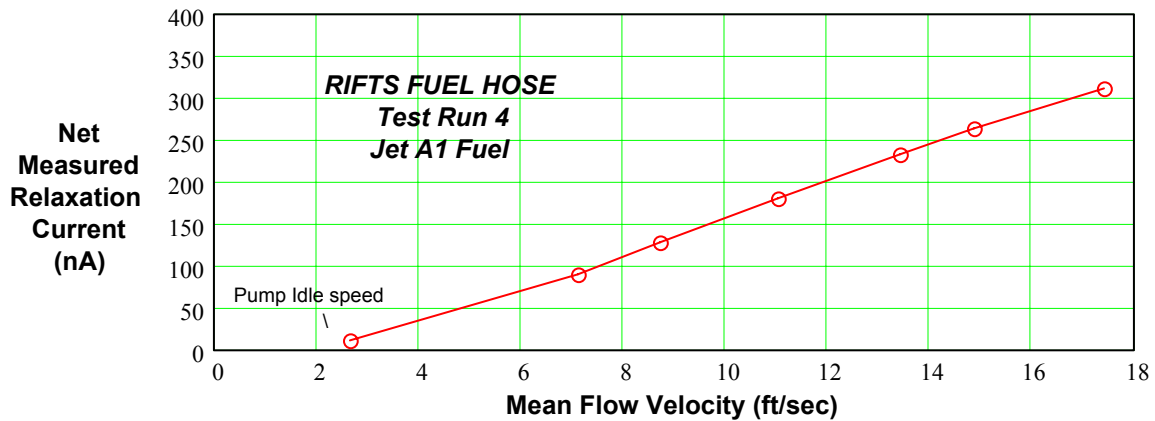


Figure 34. Net Relaxation Current in RIFTS Hose – Test Run 4 (Aug. 2006)

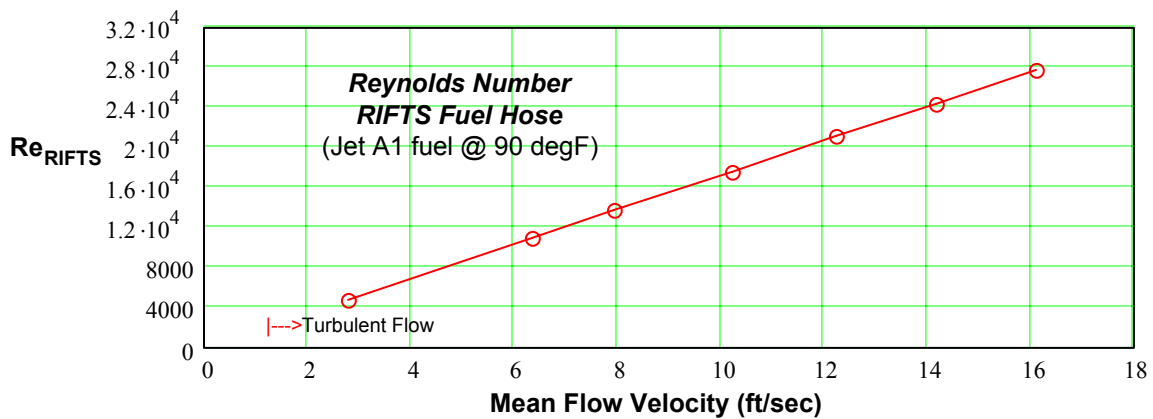
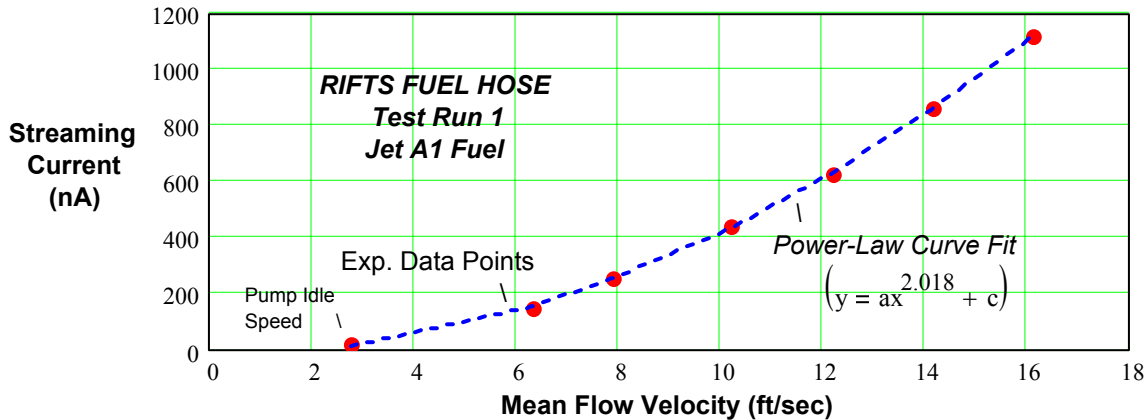
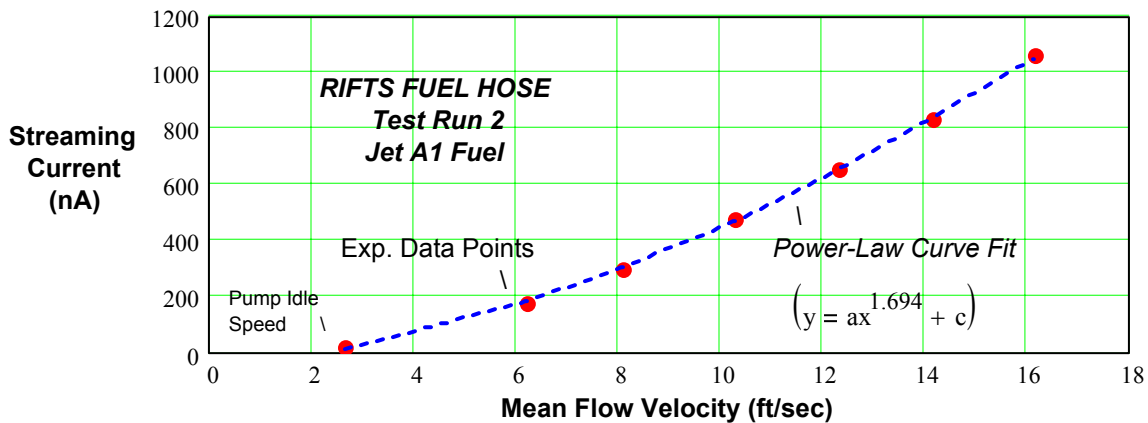


Figure 35. Reynolds Number – RIFTS Hose, Jet A1 Fuel – (Aug. 2006)

Figure 36 through Figure 39 show the corrected streaming currents together with least squares power-law curves fitted to the experimental data points. The fact that the functional dependence of streaming current on flow velocity differs for turbulent flow and for laminar flow (below about 2 ft/sec), the fitted curves have an offset relative to the  $v_f = 0$  origin. The best fit power-law exponent for the two test runs is in the range of 1.70-2.02; values that are acceptably close to the theoretical square-law dependence postulated in the earlier analysis.



**Figure 36. Streaming Current in RIFTS Fuel Hose – Test Run 1 (Aug. 2006)**



**Figure 37. Streaming Current in RIFTS Fuel Hose – Test Run 2 (Aug. 2006)**

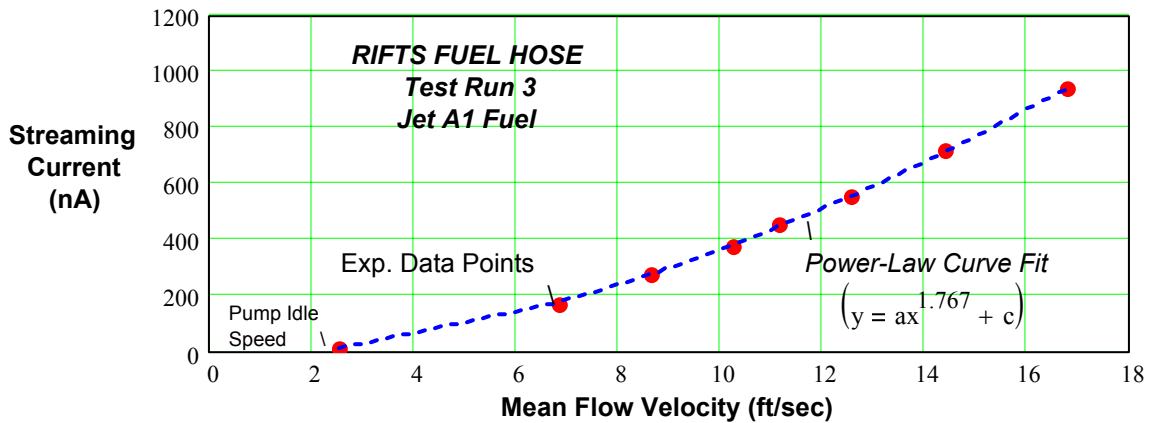


**Figure 38. Streaming Current in RIFTS Fuel Hose – Test Run 3 (Aug. 2006)**

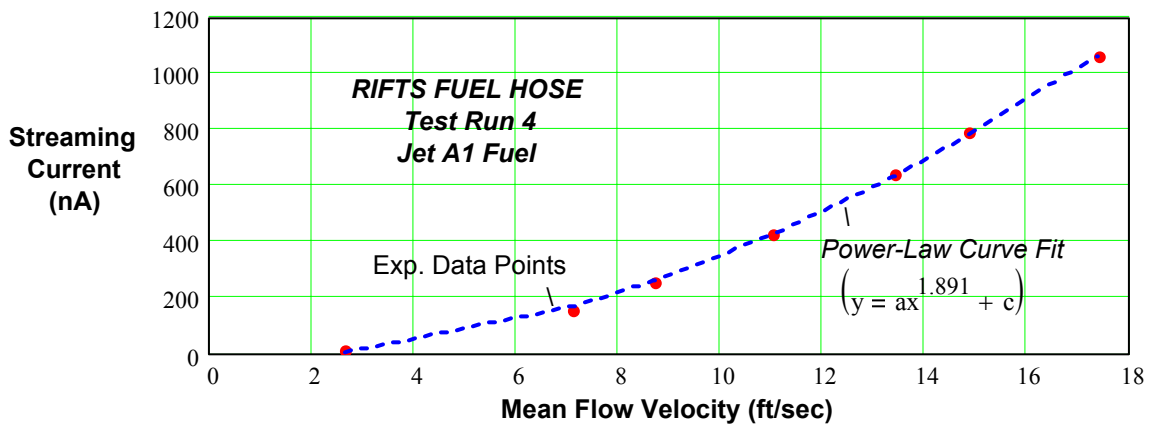


**Figure 39. Streaming Current in RIFTS Fuel Hose – Test Run 4 (Aug. 2006)**

Figure 40 presents the triboelectric charging coefficient,  $B_{TT}$ , for the RIFTS fuel hose. Since the four test runs were performed at preset flow velocity increments, the average value curve shown in Figure 40 is the mean value of  $B_{TT}$  for the four test runs plotted versus the mean values of flow velocity at each measurement point.

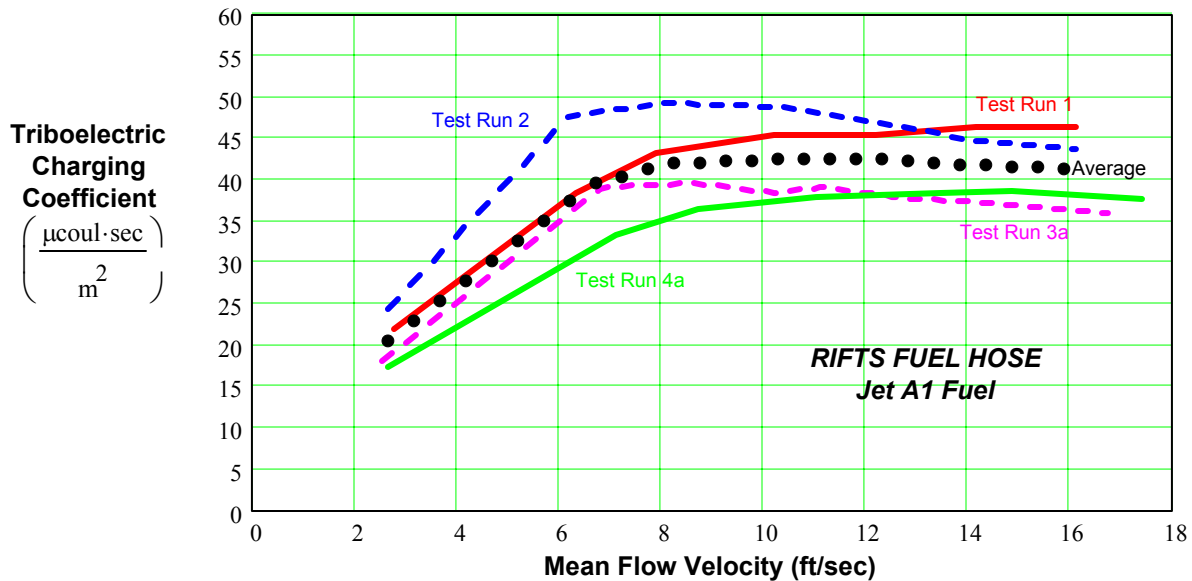
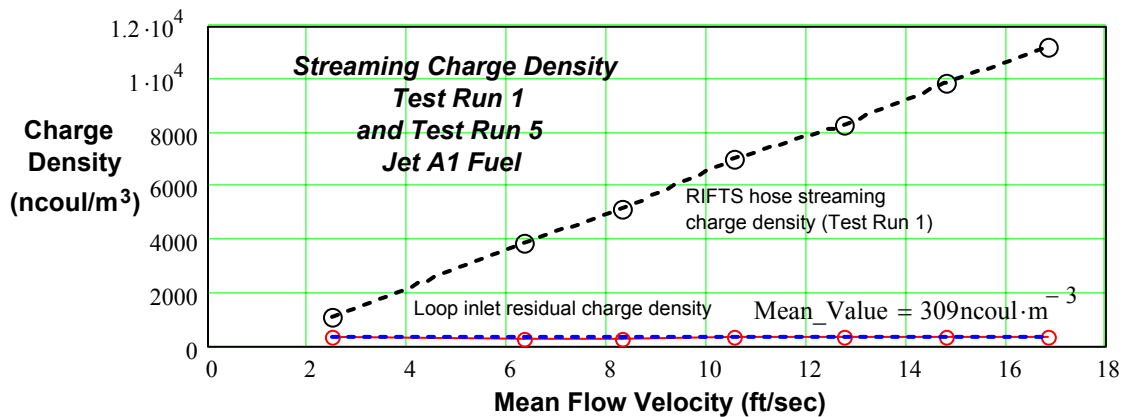


Figure 40. Triboelectric Charging Coefficient – RIFTS Fuel Hose (Aug. 2006)

### 7.1.2.2 Fuel Flow Loop Checkout Test

An important electrostatic consideration in the design of the fuel flow loop was the potential generation of extraneous static charge in the fuel by the ancillary parts of the loop system such as the pump, fuel reservoir bladder, connecting hoses, and connecting fittings. The residual charge entering the hose test section was determined by installing the two streaming current measurement sections in cascade at the immediate outlet of the upstream relaxation vessel. In this test, the upstream measuring section serves as a reference stage for the downstream measuring section so that the total electrostatic charge entering the hose test section may be determined. Although the different possible sources of any such residual charge cannot be determined, the objective of the test is to determine that the magnitude of the charge produced by the ancillary parts of the fuel circulation system is sufficiently small as to be negligible or otherwise known and accounted for in the data analysis. As discussed in connection with Equation (10), the ratio of the relaxation currents measured as a function of the fuel flow velocity provides a means for deriving the residual static charge density entering the hose test section. Figure 41 shows the residual charge density measured versus flow velocity at the end of the various streaming current tests. Also shown in this figure is a plot of the streaming charge density derived from the streaming current measured in Test Run 1 (Figure 36), showing that the residual charge is quite small and relatively independent of fuel flow.



**Figure 41. Residual Charge Density Entering the Hose Test Section**

### 7.1.2.3 Electrostatic Potential Measurements on the RIFTS Fuel Hose

Electrostatic potential measurements were performed on the RIFTS hose simultaneously with the streaming current measurements although not all of the test runs yielded productive test data because of wet hose conditions and inadequate hose isolation support due to wetness. The hose potential tests consisted of:

- (1) electric field meter calibration;
- (2) field meter readings at fixed positions on the hose versus fuel flow rate; and
- (3) field meter readings at fixed fuel flow rates versus position along the hose.

These tests were performed on two successive days with overnight rain limiting the measurements on the second day to only afternoon tests halted by the onset of light rain after four hours of work. Field meter measurements on the first day yielded the highest hose potential values and tests on the second day characterized the potential at various selected positions along the hose versus flow rate. The tests on the second day served mainly to demonstrate the adequacy of the hose support insulation test conditions on the two test days and to provide repeated measurements for some of the test conditions observed on the first day.

Figure 42 shows the hose potential calibration curve for measurements on the RIFTS fuel hose using the electric field meter probe installed in the grounded cylindrical metallic shell. For calibration purposes, a 36-in. long section of 6-inch diameter stainless steel pipe was placed in the shell assembly and an adjustable high-voltage power supply used to produce known steady-state electric field conditions in the 3.25-in. annular air gap. The field meter instrument was first adjusted to zero with the pipe and shell connected to ground. The high-voltage power supply was then attached from ground to the pipe and adjusted in approximate 1,000 VDC increments over its available range of 3,200-12,600 VDC to yield corresponding field meter readings. These data provided sufficient information to produce a valid curve fit for interpreting the experimental field readings obtained during the various RIFTS hose tests using the field sensor probe and grounded shell at an annular air gap of 3.0 in. The field meter instrument and testing

arrangement exhibited a calibration sensitivity factor of 1.709 applied to the annular air gap spacing (7.62 cm) between the RIFTS hose and the grounded metal shell and a bias offset voltage of -217.4 volts when adjusting the measured field meter readings to calculate the supported hose potential. The experimentally derived calibration equation for the potential of the supported RIFTS hose is

$$V_{RIFTS} = 1.709 \cdot g_{RIFTS} \cdot E_{FM} - 217.4 \text{ volts} \quad (31)$$

where:  $g_{RIFTS}$  = Annular air gap between the hose and the grounded cylindrical metallic shell; and

$E_{FM}$  = Experimentally measured electric field.

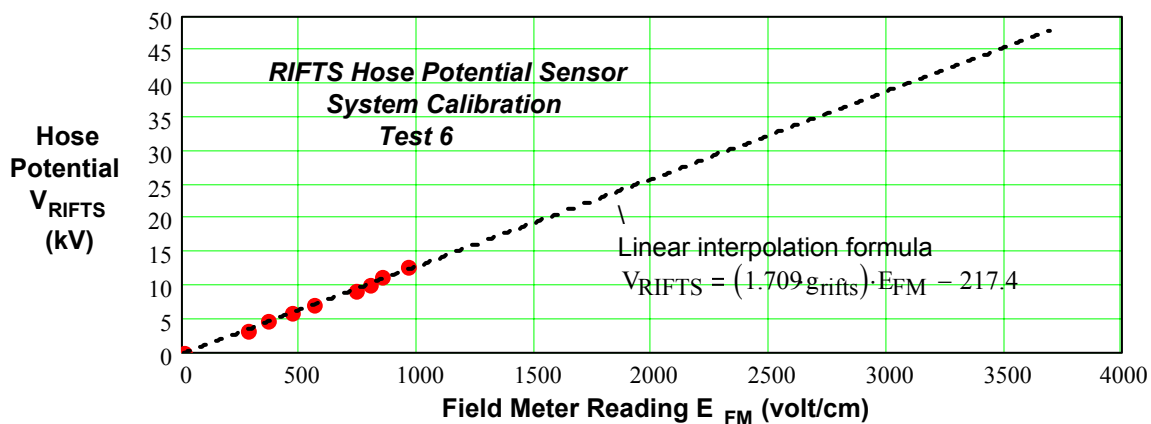


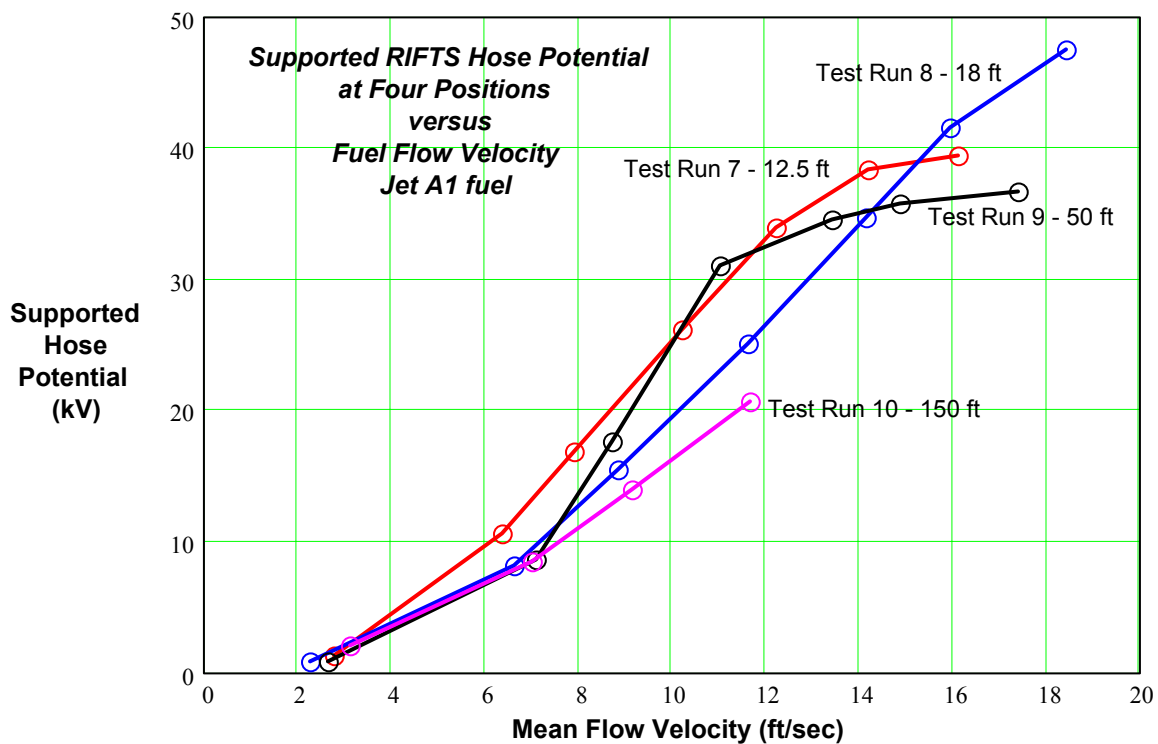
**Figure 42. Field Meter Calibration Curve for Potential Measurements on the RIFTS Fuel Hose**

Potential measurements were made along the RIFTS hose beginning at the inlet to the hose test section and progressing toward the end of the hose. The electric field sensor in combination with the grounded cylindrical metal shell provided reliable field measurements that could be converted to potential readings using the analytical methods described earlier and represented by the experimental calibration curve shown in Figure 42. During the field tests, comparisons of field readings with and without the lower half of the grounded shell showed that the lower half could be eliminated without affecting the readings, thus allowing a simpler way to move the sensor system along the hose.

The initial potential measurements revealed that the PVC isolators were apparently conductive enough to cause a distributed voltage drop along the hose. By reducing the number of supports, cleaning dust and dirt from the supports, and placing clean dry paper pads between the hose and the supports, the isolation was improved. These preparations were successful in achieving good isolation of the hose as evidenced by the relatively uniform potential along the full length of the hose. The hose potential was thereafter observed to increase with increasing fuel flow with relatively fast response. When the fuel flow was decreased the hose potential decayed slowly, indicating that the build-up and decay processes are governed by different time constants. The

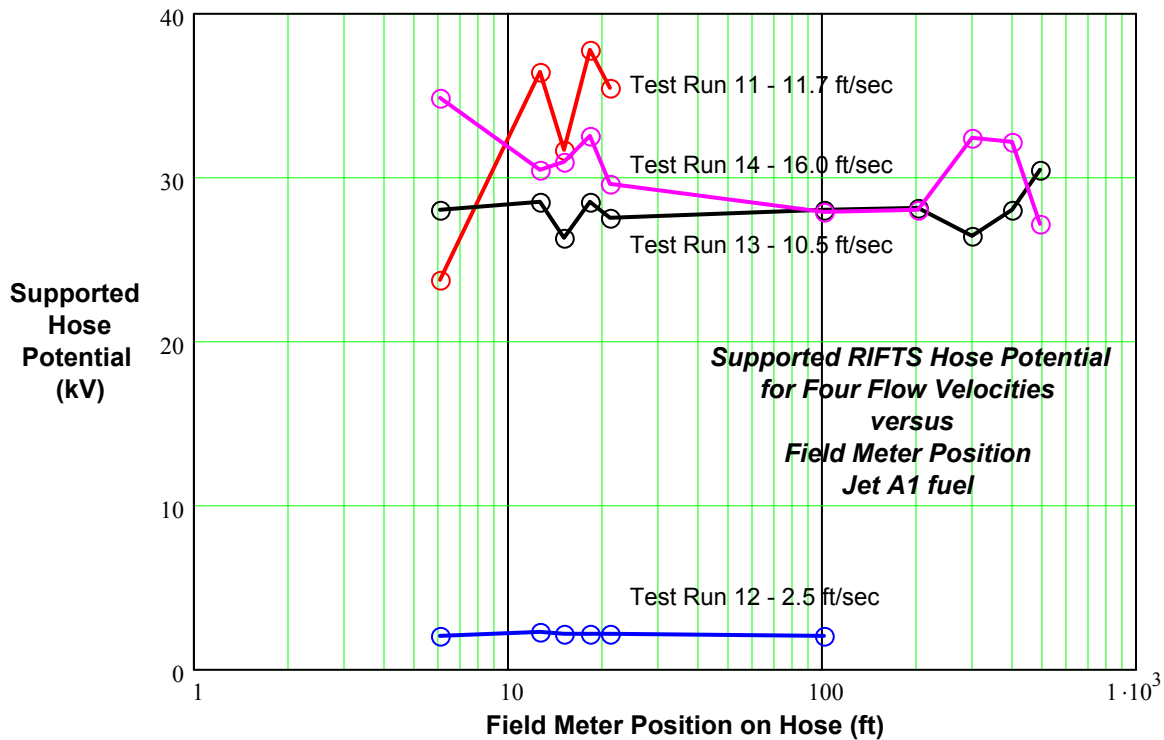
former is related directly to the triboelectric charging of the fuel whereas the latter is dependent on the insulating qualities of the hose isolator supports.

Figure 43 shows the calibrated RIFTS hose potential observed during two different days of field-testing. The fuel flow velocity in these tests ranged from a minimum of 2 ft/sec to a maximum of about 18 ft/sec and the highest potential was observed to be 47.4 kV at a fuel flow velocity of 18.4 ft/sec in Test Run 8. Test Run 7 and Test Run 9, conducted on different days, show the highest hose potentials at the lower fuel flow velocities in which the maximum potential was about 26 kV. The hose potentials observed at a fuel flow velocities of 8-9 ft/sec are observed to be about 16-17 kV. The highest measured hose potentials are noted to occur near the upstream end of the hose test section. The position of the field sensor is measured from the upstream end of the hose and in Figure 43 these distances are 12.5, 18, 50, and 150 feet.



**Figure 43. Electrostatic Potential at Four Test Positions on the RIFTS Flexible Fuel Hose**

Figure 44 shows the supported RIFTS hose potential measured at up to ten positions on the hose during four fixed fuel flow velocity conditions recorded on two successive days. The highest potentials occur at the upstream end of the hose test section and are typically in the range of about 30-35 kV for fuel flow velocities of 10.5 ft/sec and higher, taking into account the scatter in the data. The measurements in Test Runs 12 – 14 were performed on the second day of the tests following an overnight rain that wetted the hose and its PVC isolator supports. Collectively, the test results of Test Runs 7-10 shown in Figure 43 are consistent with the results for Test Runs 11-14 shown in Figure 44.



**Figure 44. Electrostatic Potential along the RIFTS Hose for Four Fuel Flow Velocity Test Conditions**

**7.1.2.4 Laboratory Tests of Fuel Hose Dielectric Strength and Breakdown Voltage**

An independent testing laboratory (Plastics Technology Laboratories, Inc., Pittsfield, MA) provided standard testing of the RIFTS and AHS flexible fuel hose materials for dielectric strength and breakdown voltage (Table 3). Two tests were performed on the RIFTS hose: (1) Samples of new hose material, and (2) Samples of hose material that had been deployed in previous field tests at Yuma Proving Ground. Tests on the AHS hose utilized samples of new hose material. The test results listed below are the average values obtained from tests on five samples of each hose. The laboratory tests were performed at room temperature using dry hose samples placed in an oil medium to prevent premature breakdown.

**Table 3. Fuel Hose Dielectric Strength and Breakdown Voltage**

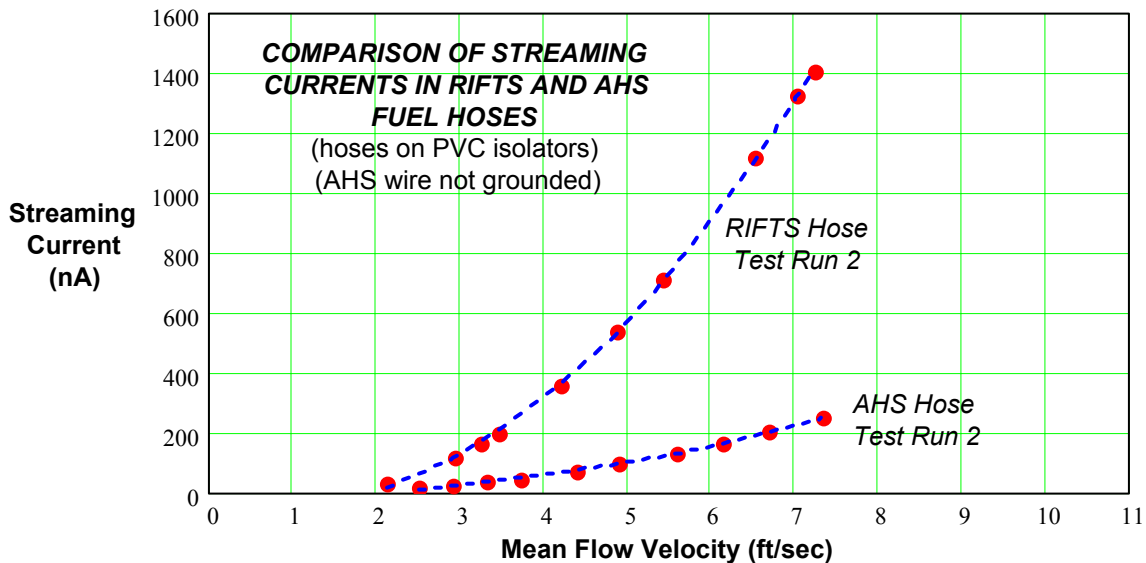
Hose Type	Sample Thickness (in)	Breakdown Voltage (kV)	Dielectric Strength (kV/in)
RIFTS – New	0.396	34.9 (Std Dev: 7.4)	88 (Std Dev: 19)
RIFTS – Used	0.409	39.6 (Std Dev: 3.7)	96.7 (Std Dev: 9.2)
AHS – New	0.144	48.3 (Std Dev: 1.7)	336 (Std Dev: 23)

## 7.2 Discussion of Field Test Results

### 7.2.1 Streaming Current Tests

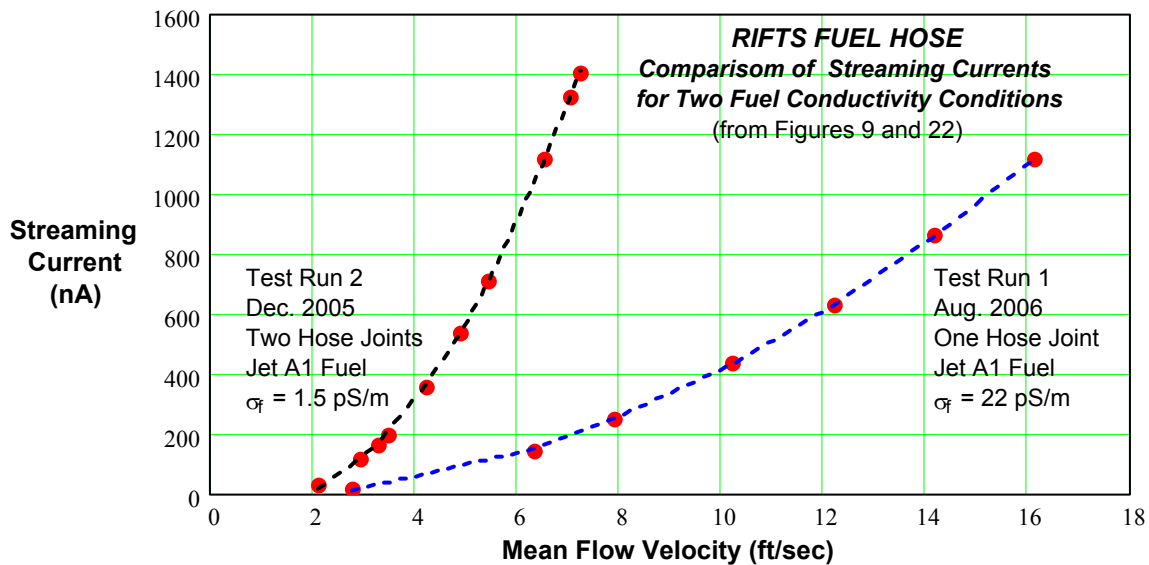
The field tests performed in December 2005 and in August 2006 revealed significant electrostatic charging effects in the RIFTS and AHS flexible fuel hoses. The streaming current measurements in both series of tests were similar for the two types of hoses, with the RIFTS hose exhibiting streaming currents about six times higher than those in the AHS hose for the same fuel flow velocities (Dec. 2005 tests). This difference is primarily attributable to the different hose wall materials in contact with the fuel and the roughness of their inner wall surfaces. The measured streaming currents were found to be in reasonable agreement with the theoretical model characteristics for turbulent fuel flow in which streaming current is approximately proportional to the square of flow velocity (streaming charge density linearly proportional to flow velocity) together with added influences by the fuel dielectric constant and electrical conductivity (i.e., the fuel relaxation time constant). Triboelectric charging coefficients were derived from the experimental data to allow the streaming currents to be predicted on future occasions when using the same types of hoses under similar field testing conditions.

Figure 45 shows representative measurements of electrostatic streaming currents in the RIFTS and AHS fuel hoses recorded during the December 2005 field tests. The Jet A1 fuel used in these tests had an electrical conductivity of 1.5 pS/m and the fuel temperature during the tests was approximately 35°F. The AHS hose exhibits lower electrostatic charging than the RIFTS hose by a factor of approximately 6.1.



**Figure 45. Comparison of Streaming Currents Generated in the RIFTS and AHS Flexible Fuel Hoses (Dec. 2005 Tests)**

Although there were physical differences in the fuel flow loop setups used in December 2005 and in August 2006, the primary difference in the tests was in the electrical conductivity of the Jet A1 fuel. The fuel conductivity in December 2006 was 1.5 pS/m and, after seven months of on-site storage, the conductivity increased to 22 pS/m. Figure 46 shows a comparison of representative streaming currents in the RIFTS hose as recorded during the two series of tests. The increase in fuel conductivity by a factor of 14.7 reduced the streaming current by a factor of approximately 6.2 over the flow velocity range for which the test results could be compared.



**Figure 46. Comparison of Streaming Currents in the RIFTS Hose Tests Conducted in December 2005 and in August 2006**

The change in fuel conductivity provided the opportunity to use the fuel flow model derived for the RIFTS hose in the first series of tests as a basis for predicting the streaming current in the second series of tests. Figure 47 shows a comparison between the measured and predicted streaming currents for Jet A1 fuel having a conductivity of 22 pS/m. The predicted values are approximately 18 to 37 percent lower than the measured values, depending on the fuel flow velocity. This velocity dependence implies that an additional functional dependency on flow is not accounted for in the postulated triboelectric charge separation model. In particular, the present model does not account for the boundary flow effects dependent on fuel temperature (i.e., the fuel viscosity and its effect on Reynolds number) as well as possible molecular level effects on fuel charge separation in the presence of the small moisture diluent causing the increase in conductivity. A more complete understanding of this error will require further tests using fuels having a representative range of electrical conductivities and temperatures.

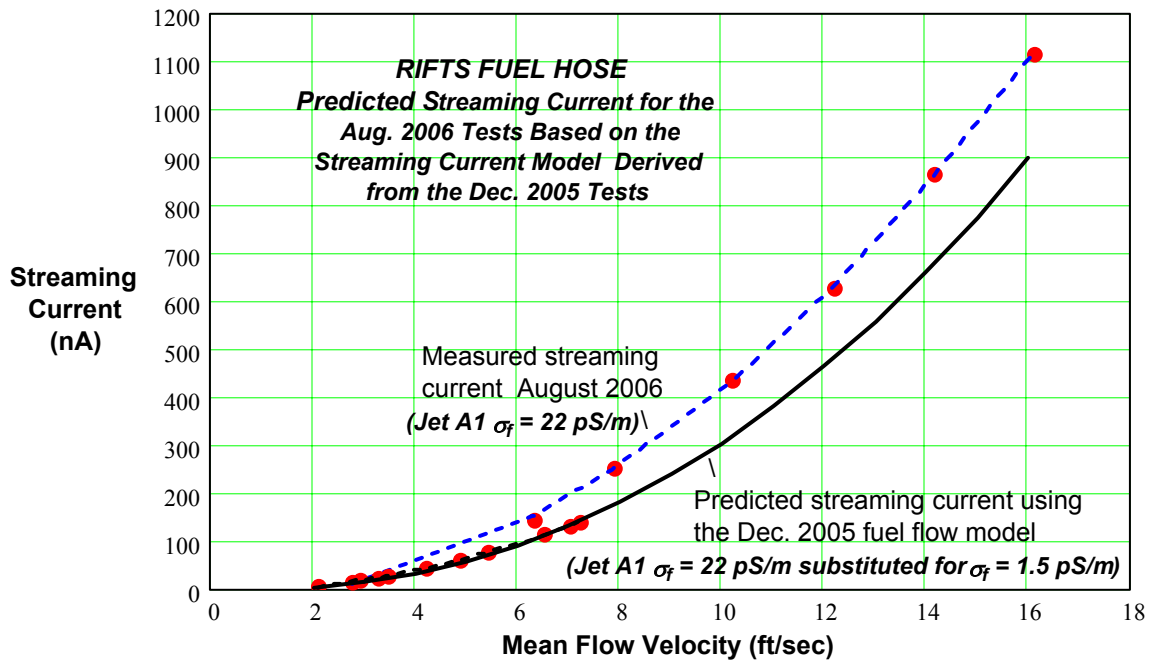


**Figure 47. Measured and Predicted Streaming Current in the RIFTS Hose for the Change in Fuel Conductivity**

### 7.2.2 Electrostatic Hose Potential Tests

The primary purpose of the Fort Lee field tests was to obtain meaningful measurements of the electrostatic potential developed on the RIFTS fuel hose when transporting hydrocarbon fuel. More specifically, the goal of the tests was to determine the highest potential generated as a function of fuel flow so that the hazardous conditions related to electrical breakdown of the hose wall could be assessed. For this purpose, the measurements required the hose to be supported on high quality insulators to allow an image electrostatic charge equivalent in magnitude to that produced internally in the hose to accumulate on the outer surface. Thus, the quality of the insulating supports together with the prevailing atmospheric environmental conditions had a direct influence on the indicated hose potential. The hose potential was measured by a calibrated non-contacting electric field sensor designed to fit the RIFTS hose. Under normal operating conditions, the hose would be laid on the ground and the image charge would be concentrated in the earth immediately under the hose and, therefore, the hose potential would appear only across the hose wall thickness and not be measurable by the field sensor. The PVC isolators used in the tests served only to facilitate the measurement of the hose potential associated with the external surface charge

Knowledge of the hose potential provides practical information on the dielectric stress across the hose wall when the hose is placed on the ground or when a grounded metal object comes in contact with the hose. With close attention to the hose insulation conditions and by avoiding anyone or anything touching the supported hose, successful measurements of high potential were

obtained during the August 2006 field tests. In these tests, field sensor readings were recorded at various positions along the hose to evaluate the distributed resistance associated with the PVC isolator supports and to determine the position at which the maximum potential occurred. Figure 44 shown earlier illustrates the potential to be relatively uniform along the full length of the hose during the two days on which the potential measurements were performed. The highest measured potentials were in the range of 40 – 48 kV at positions within the first 20 feet of the test hose section and at flow velocities of 16 ft/sec and 18 ft/sec, respectively (Figure 43, Test Runs 7 and 8). The variations in hose potential shown in Figure 43 are associated with changes in the PCV support resistances caused by movements of the hose induced by changes in hose pressure and the dynamic effects of fuel flow inertia in curved sections of the hose with increasing fuel flow during each test run.

The worst-case RIFTS hose potentials of particular interest are those recorded at fuel flow velocities of about 12 ft/sec and lower as shown in Test Runs 7, 8 and 11 in Figure 46 and Figure 47. At the flow velocity of 12 ft/sec (1,129 gpm) the observed hose potential was in the range of 35 – 38 kV. However, the maximum emergency fuel flow rate for the RIFTS hose is 800 gpm (8.50 ft/sec) and the nominal flow rate is 600 gpm (6.38 ft/sec) for which the observed worst-case hose potentials were approximately 20 kV and 10 kV, respectively. The experimentally established breakdown potential for the RIFTS hose listed in Table 3 is  $34.9 \text{ kV} \pm 7.4 \text{ kV}$  at 95 percent confidence level for new hoses and  $39.6 \text{ kV} \pm 3.7 \text{ kV}$  at 95 percent confidence level for well used hoses. Therefore, for new RIFTS hoses, the electrostatic potential would not be expected to be greater than about 57 percent of the established breakdown voltage under emergency fuel flow conditions and not greater than about 29 percent of the breakdown voltage under nominal fuel flow conditions. When considering the breakdown voltage for used RIFTS hoses, the electrostatic potential would not be greater than about 51 percent of the breakdown voltage under emergency fuel flow conditions and not greater than about 25 percent of the breakdown voltage under nominal fuel flow conditions. These hose potential levels appear to be adequately safe for both new and used hose conditions for the present RIFTS hose design since fuel flow rates of more than 12 ft/sec involving fuels having an electrical conductivity as low as 22 pS/m are required before the hose potential might be comparable with the hose breakdown rating.

## **8.0 CONCLUSIONS AND RECOMMENDATIONS**

### **8.1 Summary**

Full-scale fuel flow tests were performed in December 2005 and in August 2006 to demonstrate and evaluate the electrostatic charging effects in the RIFTS and AHS flexible fuel hoses. These tests were successful in demonstrating the relative streaming currents in both types of hose and the associated electrostatic potential on the RIFTS hose. Inclement weather conditions prevented potential measurements on either hose types during the December 2005 tests and the August 2006 field tests were devoted exclusively to tests on the RIFTS hose. The maximum experimental fuel flow velocities obtained in the December 2005 tests were limited to about 7 ft/sec for the RIFTS hose and about 10 ft/sec for the AHS hose. In planning the August 2006

field tests, changes were made in the flow loop setup to provide fuel flow velocities up to about 18 ft/sec, which is substantially above the average velocity of 8.5 ft/sec obtained within the RIFTS hose when operating at emergency flow conditions of 800 gpm.

The measured streaming currents were in reasonably good agreement with the postulated theory for triboelectric charging in non-conducting plastic hoses. The December 2005 streaming current tests revealed distinct differences between the RIFTS and the AHS hoses, with the AHS hose exhibiting only about one-sixth of the streaming current observed in the RIFTS hose. The Jet A1 fuel used in the December 2005 tests had an electrical conductivity of 1.5 pS/m, representing a fuel having the highest available electrostatic activity. The August 2006 tests were performed only on the RIFTS hose under conditions where the electrical conductivity of the same Jet A1 fuel used in December 2005 increased from 1.5 pS/m to 22 pS/m. This change in conductivity reduced the RIFTS hose streaming current by a factor of 6.2.

Six definitive tests runs were conducted in August 2006 to measure and evaluate the electrostatic potential developed on the RIFTS hose during fuel flow. The measured maximum potential during these tests was 48 kV at a fuel flow velocity of 18 ft/sec. When the observed hose potential is constrained to the RIFTS hose fuel velocity design limits, the indicated worst-case potential was 20 kV at the maximum emergency flow rate of 800 gpm (8.50 ft/sec) and 10 kV at the nominal flow rate of 600 gpm (6.38 ft/sec). Independent test laboratory measurements established the breakdown voltage of the RIFTS hose to be 34.9 kV at 95 percent confidence level for new hose material and 39.6 kV for used hose material; values that are 1.75 times higher and 1.98 times higher, respectively, than the value measured at the rated RIFTS maximum emergency fuel flow velocity.

## 8.2 Conclusions

The electrostatic potentials observed on the RIFTS hose, at its specified flow ratings, when carrying Jet A1 fuel having an electrical conductivity of 22 pS/m are:

RIFTS Maximum Emergency Flow Rate (800 gpm; 8.50 ft/sec) . . .	20 kV
RIFTS Nominal Flow Rate (600 gpm; 6.38 ft/sec) . . . . .	10 kV

These hose potentials are considered to be adequately safe for RIFTS hose deployment and operation under all practical field conditions, particularly when the transported fuel has a minimum electrical conductivity of 22 pS/m, or higher.

The AHS flexible fuel hose has a metallic wire braid molded onto its outer surface to serve as a continuous grounded wire along the entire hose length. This wire provides a self-contained method of grounding the outer surface of the hose, supplementing the presence of the earth ground on which the hose is laid. Although no potential measurements were possible on the AHS hose because of unfavorable field conditions in December 2005, the presence of the molded-on wire would have affected the hose potential in different ways depending on whether the wire was grounded or ungrounded to earth. However, since the external wire only tends to suppress the image charge that accumulates on the outer surface of the hose, the separated bound

charge on the inner surface of the hose and the streaming counter-polarity charge flowing in the fuel are still present in the interior of the hose. For this reason, there will still be an electrostatic potential developed across the hose wall when the hose is deployed on the ground. This is true for both the AHS and RIFTS hose as well as for any conduit flowing a hydrocarbon fuel. Therefore, in view of the relatively low electrostatic charging effects expected under normal and emergency operation of the RIFTS hose, the use of such a molded-on ground braid wire on the RIFTS hose appears to offer no advantage in reducing the dielectric stress across the hose wall.

Two types of hose construction were investigated. Each had its own physical characteristics of interior surface roughness, construction technique (extruded through the weave or multi-jacketed), and materials of construction. These features influence the derived Triboelectric Charging Coefficient,  $B_{TT}$ , which conveys considerable information about the electrical performance of the hose. Knowledge of this parameter is useful in predicting streaming current and can be used as a reference parameter for comparing hoses.

### 8.3 Recommendations for Future Work

1. Extend the theoretical triboelectric charging model for non-conducting plastic hoses to include an analytical relationship for predicting the electrostatic potential on the hose based only on knowledge of the fuel electrical properties and the fuel flow velocity in the RIFTS hose. Check the validity of the model hose potential predictions against the RIFTS hose measurements recorded at Fort Lee, VA in August 2006.
2. Conduct experimental tests of the AHS flexible fuel hose (hose length: ~ 100 ft) to characterize the electrostatic potential developed on the hose.
3. Perform laboratory tests to destructively determine the dielectric strength and breakdown voltage of the RIFTS hose and the AHS hose under simulated conditions of pressured fuel transport and different external hose grounding conditions (water substituted for fuel). This can be accomplished with short lengths of isolated hose set upon a benchtop test rig.
4. Refine the triboelectric charging model applicable to non-conducting fuel hoses to more accurately account for fuel temperature effects and molecular charge separation effects in fuels containing moisture and other additives affecting the fuel electrical conductivity.
5. Conduct Laboratory-scale triboelectric charging tests on experimental non-conducting fuel hoses made of different materials, including conducting polymer materials, and different hose wall roughness conditions to derive new hose design specifications that minimize electrostatic charging effects in all military fuels or otherwise permit higher fuel transport flow rates. This work would yield a table of triboelectric charging coefficients for a variety of hoses.

## 9.0 REFERENCES

- Gibson, N., (1971). "Static in Fluids," *Static Electrification - 1971*; Paper 9, pp. 71 - 83.
- Hearn, G.L. and Jones, R.T. (1991). "*Electrostatic Hazards Associated With the Use of Flexible Plastic Hoses*," Rpt. No. 139RJ, Wolfson Engineering Consultancy, Univ. of Southampton, Southampton, England.
- Leonard, J.T. and Carhart, H.W., (1969). *U.S. Naval Research Laboratory Report No. 6952*.
- Leonard, J.T. and Carhart, H.W., (1971). "*Static Electricity Measurements During Refueler Loading*," *U.S. Naval Research Laboratory Report No. 7203*.
- Schön, G. (1965). *Handbuch der Raumexplosionen*; H.H. Freytag, Ed., Weinheim Bergstr., Verlag Chemie.
- Touchard, G. (1978). "Streaming Currents Developed in Laminar and Turbulent Flows Through a Pipe," *J. Electrostatics*, Vol. 5 pp. 463-478.
- Touchard, G. (2001). "Flow Electrification of Liquids," *J. Electrostatics*, Vol. 51-52, pp. 440-447.
- Vazquez-Garcia, J., et al. (2005). "A Critical Approach to Measure Streaming Current: Case of Fuels Flowing through Conductive and Insulating Polymer Pipes," *IEEE Trans. Ind. Appl.*, Vol. 41, No. 5, pp. 1335-1342.
- Walmsley, H.L. (1996). "The Electrostatic Fields and Potentials Generated by the Flow of Liquid Through Plastic Pipes," *J. Electrostatics*, Vol. 38, pp. 249-266.
- Walmsley, H.L. and Woodford, G. (1981). "The Generation of Electric Currents by the Laminar Flow of Dielectric Liquids," *J. Phys. D: Applied Phys.*, Vol. 14, pp. 1761-1782.

## 9.1 SUPPLEMENTAL REFERENCES

### *American Society for Testing and Materials:*

- D 1655 "*Specifications for Aviation Turbine Fuels*," Annual Book of ASTM Standards Vol. 05.01.
- D 2624 "*Test Methods for Electrical Conductivity of Aviation and Distillate Fuels*," Annual Book of ASTM Standards Vol. 05.02.
- D 4308 "*Test Method for Electrical Conductivity of Liquid Hydrocarbons by Precision Meter*," Annual Book of ASTM Standards Vol. 05.02.
- D 4865-97 "*Standard Guide for Generation and Dissipation of Static Electricity in Petroleum Fuel Systems*," ASTM Committee D-2, Subcommittee D02.J (Aviation Fuels), August 1997. [Supercedes D4865-96].

***Coordinating Research Council, Inc.(Atlanta, GA):***

- (1994) “*The Effect of Aviation Fuels Containing Small Amounts of Static Dissipator Additive on Electric Charge Generation,*” CRC Report No. 590, 1994.
- (1993) “*Aircraft and Refueler Bonding and Grounding Study,*” CRC Proj. No. CA-36-61, CRC Aviation Electrical Discharge Group, February 1993.

***National Research Council of Canada:***

- (1983) Gardner, L. and Moon, F.G., “*The Relationship Between Electrical Conductivity and Temperature of Aviation Turbine Fuels Containing Static Dissipator Additives,*” NRC Report No. 22648, 1983.

***Society of Automotive Engineers:***

- (1984) “*Minimization of Electrostatic Hazards in Aircraft Fuel Systems,*” Aerospace Information Report AIR-1662, SAE Committee AE-5, October 1984.